UNIVERSIDADE ESTADUAL DE MARINGÁ
Centro de Ciências Biológicas
Programa de Pós-Graduação em Ciências Biológicas
Área de Concentração: Biologia Celular e Molecular

HÉLITO VOLPATO

AVALIAÇÃO BIOLÓGICA E ELUCIDAÇÃO DO MECANISMO DE AÇÃO DO COMPOSTO SINTÉTICO 4-[(2*E*)-*N*'-(2,2'-BITIENIL-5-METILENO)HIDRAZINACARBONIL]-6,7-DIIDRO-1-FENIL-1*H*-PIRAZOLO[3,4-*d*]PIRIDAZIN-7-ONA SOBRE *Leishmania* sp.

Maringá

2018

HÉLITO VOLPATO

AVALIAÇÃO BIOLÓGICA E ELUCIDAÇÃO DO MECANISMO DE AÇÃO DO COMPOSTO SINTÉTICO 4-[(2*E*)-*N*'-(2,2'-BITIENIL-5-METILENO)HIDRAZINACARBONIL]-6,7-DIIDRO-1-FENIL-1*H*-PIRAZOLO[3,4-*d*]PIRIDAZIN-7-ONA SOBRE *Leishmania* sp.

Tese apresentada ao Programa de Pós-Graduação em Ciências Biológicas (Área de concentração – Biologia Celular e Molecular) da Universidade Estadual de Maringá, para obtenção do grau de Doutorado em Ciências Biológicas.

Orientador: Prof. Dr. Celso Vataru Nakamura
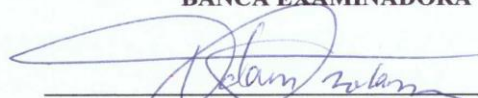

Maringá

2018

HÉLITO VOLPATO

AVALIAÇÃO BIOLÓGICA E ELUCIDAÇÃO DO MECANISMO DE AÇÃO DO COMPOSTO SINTÉTICO 4-[(2*E*)-*N*'-(2,2'-BITIENIL-5-METILENO)HIDRAZINACARBONIL]-6,7-DIIDRO-1-FENIL-1*H*-PIRAZOLO[3,4-*d*]PIRIDAZIN-7-ONA SOBRE *Leishmania* sp.

Tese apresentada ao Programa de Pós-Graduação em Ciências Biológicas (Área de concentração – Biologia Celular e Molecular) da Universidade Estadual de Maringá, para obtenção do grau de Doutorado em Ciências Biológicas.

Orientador: Prof. Dr. Celso Vataru Nakamura
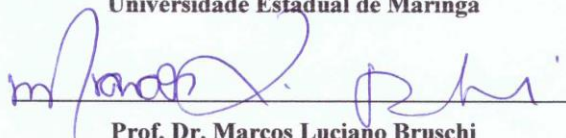
Aprovado em: 24/04/2018

BANCA EXAMINADORA

Prof. Dr. Celso Vataru Nakamura
Universidade Estadual de Maringá

Prof.ª Dr.ª Sueli Fumie Yamada Ogatta
Universidade Estadual de Londrina

Prof.ª Dr.ª Fernanda Andréia Rosa
Universidade Estadual de Maringá

Prof. Dr. Marcos Luciano Bruschi
Universidade Estadual de Maringá

Prof. Dr. Rodrigo Polimeni Constantin
Universidade Estadual de Maringá

BIOGRAFIA

Hélito Volpato nasceu em Amambaí/MS em 24 de outubro de 1990. Possui graduação em Ciências Biológicas (Licenciatura) pela Universidade Paranaense (UNIPAR) campus Paranavaí, Paraná (2007). Durante a graduação realizou pesquisa envolvendo sistema nervoso entérico e cardiovascular de ratos em processo de envelhecimento. Possui mestrado em Ciências Biológicas (área de concentração em Biologia Celular e Molecular) pela Universidade Estadual de Maringá. Dedicou-se desde o início do mestrado (2012) ao estudo de compostos biologicamente ativos frente a protozoários da família dos Tripanosomatídeos: *Leishmania amazonensis*, *Leishmania infantum* e *Trypanosoma cruzi*. Realizou doutorado-sanduíche na Faculdade de Farmácia da Universidade de Coimbra (FFUC), Coimbra, Portugal, no laboratório de Tecnologia Farmacêutica e Laboratório de Parasitologia sobre supervisão da Prof.ª Dr.ª Maria do Céu Sousa e Prof.ª Dr.ª Olga Borges.

APRESENTAÇÃO

Esta tese é composta por dois artigos científicos contemplando os resultados obtidos durante as duas etapas do doutorado. Em consonância com as regras do Programa de Pós-Graduação em Ciências Biológicas, ambos os artigos foram escritos e, posteriormente serão publicados em periódicos que atenda aos critérios vigentes estabelecidos pela CAPES.

O primeiro artigo relata os resultados obtidos no laboratório de Inovação Tecnológica no Desenvolvimento de Fármacos da Universidade Estadual de Maringá. O artigo, intitulado "Activity of the pyrazolo [3,4-*d*]pyridazinone-*N*-acylhydrazone-(bi)thiophene hybrid in *Leishmania amazonensis* is mediated by apoptotic and necrotic characteristics induced by oxidative stress" descreve a atividade biológica e o possível mecanismo de ação de um composto sintético sobre formas parasitaria de *Leishmania amazonensis*, protozoário causador da leishmaniose cutânea.

O segundo artigo relata os resultados desenvolvidos durante o doutorado-sanduíche na Faculdade de Farmácia da Universidade de Coimbra (FFUC), Coimbra, Portugal, realizado no período de Fevereiro de 2016 à Janeiro de 2017. O artigo, intitulado "*In vitro* anti-*Leishmania* activity of the **T6** synthetic compound encapsulated in β-(1,3)-D-glucan particles obtained from the cell wall of the yeast *Saccharomyces cerevisiae*", é constituindo por uma descrição da atividade de um composto sintético livre e encapsulado em partículas de glucano obtidos da levedura *Saccharomyces cerevisiae* e, sequencialmente, o estudo do possível mecanismo de ação em *Leishmania infantum*, protozoário causador da leishmaniose visceral.

RESUMO GERAL

1. INTRODUÇÃO

As leishmanioses são um grupo de doenças infecciosas causadas por protozoários heteroxênico do gênero *Leishmania* sp., um parasita que apresenta duas formas evolutivas distintas: promastigota e amastigota. A transmissão do parasito para o hospedeiro vertebrado, incluindo o homem, se dá principalmente por insetos vetores pertencentes à ordem Diptera, família Psychodidae, gênero *Phlebotomus* no Velho Mundo ou *Lutzomyia* no Novo Mundo e são conhecidos popularmente como mosquito palha ou birigui. Os atuais tratamentos de pacientes com leishmaniose são baseados em fármacos que demonstram algumas limitações como, por exemplo, diversos efeitos colaterais, longo período de tratamento e alguns casos de resistência. Neste contexto, estudos são de extrema importância na descoberta de novos compostos biologicamente ativos contra *Leishmania* sp., podendo ser um importante candidato no desenvolvimento de fármacos para o tratamento de pacientes com leishmaniose. Nosso grupo de pesquisa tem relatado uma promissora atividade anti-*Leishmania* de compostos naturais e sintéticos contendo núcleo tiofênico na estrutura.

Outra importante contribuição no desenvolvimento de fármacos é o processo de encapsulamento de compostos biologicamente ativos, como o uso de partículas de glucano (PG). As PG são partículas ocas e porosas composta por glucano, e podem ser extraídas da levedura *Saccharomyces cerevisiae*. Uma importante característica das PG é a facilidade dos macrófagos em realizar sua fagocitose. Isso é devido à presença de receptores de glucano na membrana plasmática das células fagocitárias, denominadas dectina-1.

Desta forma, o objetivo do trabalho foi avaliar atividade biológica e mecanismo de ação do composto sintético tiofênico 4-[(2*E*)-*N*'-(2,2'-bitienil-5-metileno)hidrazinacarbonil]-6,7-diidro-1-fenil-1*H*-pirazolo[3,4-*d*]piridazin-7-ona (**T6**) frente *L. amazonensis* e *L. infantum*, espécies causadoras da leishmaniose cutânea e visceral, respectivamente. Além disso, visto os macrófagos serem as principais células infectadas pelo parasito, outro objetivo fundamental foi realizar a encapsulação e investigar atividade biológica do **T6** em partículas de glucano frente formas amastigotas intracelulares de *L. infantum*.

Palavras chaves: *Leishmania* sp, tiofeno, *Saccharomyces cerevisiae* e partículas de glucano.

2. METODOLOGIAS

Os ensaios de atividade biológica e elucidação dos mecanismos de ação foram realizados com protozoários das espécies *L. amazonensis* e *L. infantum*. Para os ensaios de citotoxicidade utilizamos macrófagos da linhagem RAW.

O composto sintético tiofênico **4**-[(2*E*)-*N'*-(2,2'-bitienil-5-metileno)hidrazinacarbonil]-6,7-diidro-1-fenil-1*H*-pirazolo[3,4-*d*]piridazin-7-ona (**T6**) foi sintetizado pelo grupo de pesquisa da Prof.ª Dra.ª Fernanda Andréia Rosa e Prof.ª Dr.ª Maria Helena Sarragiotto do Departamento de Química da Universidade Estadual de Maringá (UEM).

2.1. Atividade biológica do T6 sobre *Leishmania amazonensis*

Para verificar o efeito antiproliferativo, formas amastigotas intracelulares foram tratadas com diferentes concentrações do **T6** por 48 h. Em seguida, as amostras foram coradas com Giemsa e a contagem realizada em microscópio de luz.

Com o objetivo de verificar o possível mecanismo de ação, formas promastigotas foram tratadas com CI_{50} e $2xCI_{50}$ e, em seguida, processadas para ensaios relacionados com diferentes tipos de morte celular (apoptose, necrose e autofagia). Para investigar um possível envolvimento do estresse oxidativo, um grupo foi pré-incubado com o antioxidante N-acetilcisteína (NAC).

2.2. Atividade biológica do T6 livre e encapsulado sobre *Leishmania infantum*

O processo de encapsulamento foi realizado em partículas de glucano extraídas da parede celular da levedura *Saccharomyces cerevisiae*. Para isso, realizamos a extração do conteúdo citoplasmático da levedura, e em seguida o encapsulamento através de vários ciclos com o objetivo de obter diferentes concentrações do **T6** nas partículas de glucano. Após a obtenção das partículas contendo **T6**, realizamos experimentos para avaliar a caracterização físico-química, e em seguida atividade biológica e citotoxicidade em *L. infantum* e macrófagos RAW, respectivamente.

Para elucidação do mecanismo de ação do **T6**, realizamos o tratamento de formas promastigotas com CI_{50} e $2xCI_{50}$, e posteriormente diversas metodologias foram aplicadas para verificar diferentes parâmetros celulares e bioquímicos.

3. RESULTADOS E DISCUSSÃO

3.1. Atividade biológica do T6 sobre *Leishmania amazonensis*

O **T6** demonstrou promissora atividade em formas intracelulares do parasito, obtendo um CI_{50} de 19,3 μM. Utilizando metodologias para elucidação do mecanismo de ação, verificamos importantes danos celulares induzidos pelo composto sintético **T6**, como o aumento dos níveis de espécies reativas de oxigênio (ERO), diminuição dos níveis de tióis reduzidos, exposição da fosfatidilserina, fragmentação do DNA, alteração na permeabilidade da membrana plasmática, aumento nos níveis de inclusões lipídicas, ativação de caspases, peroxidação lipídica, aumento dos níveis de ATP e alteração no ciclo celular. Podemos relacionar essas alterações no parasito com características de morte celular por apoptose e necrose, sendo essas provocadas devido ao estresse oxidativo.

Em relação à autofagia, o **T6** induziu um aumento dos vacúolos autofágicos em ambas às concentrações testadas. Curiosamente, verificamos uma redução de vacúolos autofágicos no grupo tratado com a maior concentração do **T6**. Essa interessante redução pode ser devido ao fato do protozoário utilizar o mecanismo de autofagia para reduzir os danos causados pelo composto, visto que na maior concentração os danos celulares foram mais elevados nos ensaios bioquímicos.

3.1. Atividade biológica do T6 livre e encapsulado sobre *Leishmania infantum*

Em formas promastigotas e amastigotas intracelulares, o **T6** livre, demonstrou promissora atividade biológica, correspondendo ao CI_{50} de 2,5 e 1,1 μg/mL, respectivamente. Em macrófagos RAW, o composto livre demonstrou um efeito citotóxico (CC_{50}: 2,8 μg/mL).

Para reduzir o efeito de citotoxicidade, decidimos realizar o encapsulamento do **T6** em partículas de glucano. Foi possível obter diferentes concentrações do composto encapsulado. A caracterização físico-química, possibilitou verificar importantes resultados que comprovam a presença do **T6** no interior das partículas de glucano, como o espectro de FT-IR e difração de raio-X. Por meio dos ensaios biológicos, verificamos uma considerável diminuição da citotoxicidade em macrófagos (CC_{50}: >152,3 μg/mL). Curiosamente, o CI_{50} da atividade antiproliferativa do **T6** encapsulado contra amastigotas intracelulares foi maior (8,2 μg/mL) em comparação ao **T6** livre.

Por meio de ensaios para elucidar o possível mecanismo de ação do **T6** no parasito, verificamos consideráveis alterações celulares, como a redução do volume celular, exposição da fosfatidilserina, aumento dos níveis de cálcio intracelular, aumento dos níveis de ERO e fragmentação do DNA. Esses resultados demonstram que a atividade do **T6** em formas promastigotas é ocasionada por características de morte celular por apoptose.

4. CONCLUSÕES E PERSPECTIVAS

- O composto sintético **T6** revelou ser ativo frente as formas parasitárias de *L. amazonensis* e *L. infantum*;

- Utilizando ensaios de mecanismo de ação, verificamos que o **T6** induziu danos celulares relacionados à morte celular por apoptose e necrose em *L. amazonensis*, e apenas apoptose em *L. infantum*;

- É possível que esses danos causados pelo **T6** nos parasitos podem estar relacionados com a indução do estresse oxidativo;

- Por meio dos ensaios de caracterização físico-química, foi verificado a presença da substância nas partículas de glucano em diferentes concentrações;

- O **T6** demonstrou uma considerável toxicidade em macrófagos, sendo esse efeito reduzido após a encapsulação em partículas de glucano;

- Desta forma, é possível concluir que o composto **T6** possui uma promissora atividade em diferentes espécies de *Leishmania* sp., e que essa atividade deve estar relacionada com eventos de morte celular por apoptose e necrose ocasionados pelo estresse oxidativo;

- Outros estudos devem ser realizados para auxiliar na compreensão do uso das partículas de glucano como meio de liberação de fármacos no tratamento de pacientes com leishmaniose.

ABSTRACT

1. INTRODUCTION

Leishmaniasis is a group of infectious diseases caused by heteroxenic protozoa of the genus *Leishmania* sp., a parasite that presents two distinct evolutionary forms: promastigote and amastigote.

The transmission of the parasite to the vertebrate host, including man, is through species of vectors related to the order Diptera, a family Psychodidae, the genus *Phlebotomus* in the Old World and *Lutzomyia* in the New World and are known as "mosquito-palha" or "birigui". The current treatments of patients with leishmaniasis are based on drugs that demonstrate some limitations, such as several side effects, long treatment period and some cases of resistance. In this context, new studies are extremely important in the discovery of new biologically active compounds against Leishmania sp., and may be an important candidate in the development of drugs for the treatment of patients with leishmaniasis. Our research group has reported promising anti-*Leishmania* activity of natural and synthetic compounds containing thiophene nucleus in the structure.

Another important contribution in the development of drugs is the process of encapsulating biologically active compounds, for example the use of glucan particles (GPs). GPs are hollow and porous particles composed of glucan, and can be extracted from yeast *Saccharomyces cerevisiae*. An important feature of GPs is the ability of macrophages to perform their phagocytosis. This is due to the presence of glucan receptors on the plasma membrane of phagocytic cells, the dectin-1.

Thus, our objective was to evaluate the biological activity and mechanism of action of the synthetic thiophene compound 4-[(2*E*)-*N'*-(2,2'-bithienyl-5-methylene) hydrazinecarbonyl]-6,7-dihydro-1-phenyl-1*H*-pyrazolo[3,4-*d*]pyridazin-7-one (**T6**) against *L. amazonensis* and *L. infantum*, species responsible for cutaneous and visceral leishmaniasis, respectively. Another objective was to realize the encapsulation and biological activity of **T6** in glucan particles against intracellular amastigote forms of *L. infantum*.

Keywords: *Leishmania* sp, thiophene, *Saccharomyces cerevisiae* and glucan particles.

2. Methodologies

The biological activity assays and elucidation of the mechanisms of action were performed with protozoa of the species *L. amazonensis* and *L. infantum*. For the cytotoxicity assays we used RAW lineage macrophages.

The synthetic thiophene compound 4-[(2*E*)-*N'*-(2,2'-bithienyl-5-methylene) hydrazinecarbonyl]-6,7-dihydro-1-phenyl-1*H*-pyrazolo[3,4-*d*]pyridazine-7-one (**T6**) was synthesized by the research group of Prof.ª Dr.ª Fernanda Andréia Rosa and Profª Drª Maria Helena Sarragiotto of the Department of Chemistry of the State University of Maringá (UEM).

2.1. Biological activity of T6 on *Leishmania amazonensis*

To verify the antiproliferative effect, intracellular amastigote forms were treated with different **T6** concentrations for 48 h. The samples were then stained with Giemsa and counted under a light microscope.

In order to verify the possible mechanism of action, promastigote forms were treated with IC_{50} and $2xCI_{50}$, and then processed for tests related to different types of cell death (apoptosis, necrosis and autophagy) and the oxidative stress. To investigate possible involvement of oxidative stress, one group was preincubated with the antioxidant *N*-acetyl-L-cysteine (NAC).

2.2. Biological activity of T6 alone and encapsulated on *Leishmania infantum*

The encapsulation process was performed on glucan particles extracted from the yeast cell wall of *Saccharomyces cerevisiae*. For this, we performed the extraction of the cytoplasmic content of the yeast by chemical process involving acid and base, and then the encapsulation through several cycles in order to obtain different concentrations of **T6** in the glucan particles. After obtaining **T6**-containing particles, we performed experiments to evaluate the physicochemical characterization, and then biological activity and cytotoxicity in *L. infantum* and RAW macrophages, respectively.

To elucidate the mechanism of action of **T6**, we performed the treatment of promastigotes forms with IC_{50} and $2xCI_{50}$, and later several methodologies were applied to verify different cellular and biochemical parameters.

3. RESULTS AND DISCUSSION

3.1. Biological activity of T6 on *Leishmania amazonensis*

T6 demonstrated promising activity in intracellular forms of the parasite, obtaining an IC_{50} of 19.3 µM. Through methodologies to elucidate the mechanism of action, we verified important cellular damages induced by the synthetic compound **T6**,

such as the increase of the levels of ROS, decrease of the levels of thiols reduced, phosphatidylserine exposure, DNA fragmentation, alteration in plasma membrane permeability, increased levels of lipid inclusions, activation of caspases, lipid peroxidation, increased ATP levels and alteration in the cell cycle. We can relate these changes in the parasite with characteristics of cell death by apoptosis and necrosis, which are caused due to oxidative stress.

About process of autophagy, **T6** induced an increase in autophagic vacuoles in both at the concentrations tested. Interestingly, we found a reduction of autophagic vacuoles in the group treated with the highest concentration of **T6**. This interesting result can be explained as a mechanism of cytoprotection of the parasite against the damages induced by the compound **T6**, because in the highest concentration tested we verified increase of the cellular damages in the biochemical tests.

3.1. Biological activity of free and encapsulated T6 on *Leishmania infantum*

In promastigote forms and intracellular amastigotes, **T6** alone demonstrated promising biologically activity, corresponding to the IC_{50} of 2.5 and 1.2 µg/mL, respectively. In RAW macrophages, the free compound demonstrated a cytotoxic effect (CC_{50}: 2.8 µg/mL).

To reduce the effect of cytotoxicity, we decided to encapsulate **T6** into glucan particles, and it was possible to obtain different concentrations of encapsulated **T6**. Through the physicochemical characterization, we verified important results that prove the presence of **T6** inside the glucan particles, such as the FT-IR spectrum and X-ray diffraction. By means of the biological tests, we verified a considerable diminution of the cytotoxicity in macrophages (CC_{50}: >152.3 µg/mL). Interestingly, the IC_{50} of the antiproliferative activity of the particles in intracellular amastigotes was higher (8.2 µg/mL) in comparison to the alone **T6**.

By means of assays to elucidate the possible mechanism of action of **T6** in the parasite, we observed considerable cellular alterations, such as reduction of cellular volume, exposure of phosphatidylserine, increase of intracellular calcium levels, increase of ROS levels and DNA fragmentation. These results demonstrate that **T6** activity in promastigote forms is caused by cell death by apoptosis.

4. CONCLUSIONS AND PERSPECTIVES

• The synthetic compound **T6** was found to be active against the parasitic forms of *L. amazonensis* and *L. infantum*;

• Through action mechanism assays, we verified that **T6** induced cell damage related to cell death by apoptosis and necrosis in *L. amazonensis*, and only apoptosis in *L. infantum*;

• We can relate that these damages caused by the **T6** in the parasites can be related to the induction of the oxidative stress;

• Through the tests of physical-chemical characterization, we verified the presence of the compound in the glucan particles, and obtained different concentrations;

• **T6** demonstrated considerable toxicity in macrophages, which is reduced after encapsulation into glucan particles;

• In this way, we can conclude that compound **T6** has a promising activity in different species of *Leishmania sp*., and that this activity must be related to events of cell death due to apoptosis and necrosis caused by oxidative stress. Finally, we can conclude that the use of glucan particles is an important tool of drug development, as we have verified a reduction of the toxicity presented by the free compound.

• Other studies should be performed to assist in understanding the use of glucan particles as a means of drug release in the treatment of patients with leishmaniasis.

ARTIGO CIENTÍFICO 01

Doutorando: Hélito Volpato

Orientador: Prof. Dr. Celso Vataru Nakamura

Activity of the pyrazolo [3,4-*d*]pyridazinone-*N*-acylhydrazone-(bi)thiophene hybrid in *Leishmania amazonensis* is mediated by apoptotic and necrotic characteristics induced by oxidative stress

Hélito Volpato[1,2], Nathielle Miranda[2], Jean Henrique da Silva Rodrigues[2], Andrey Petita Jacomini[3], Fernanda Andreia Rosa[3], Maria Helena Sarragiotto[3], Tânia Ueda-Nakamura[2] Sueli de Oliveira Silva[2], and Celso Vataru Nakamura[1,2*]

[1] Postgraduate Program in Biological Sciences, State University of Maringá, Maringá, Paraná, Brazil

[2] Laboratory of Technological Innovation in the Development of Drugs and Cosmetics, State University of Maringá, Maringá, Paraná, Brazil

[3] Chemistry of Department, State University of Maringá, Maringá, Paraná, Brazil

*Address for correspondence: Celso Vataru Nakamura, Laboratory of Technological Innovation in the Development of Drugs and Cosmetics, Block B-08, State University of Maringá, Av. Colombo 5790, CEP 87020-900, Maringá, Paraná, Brazil. Phone number: +55 44 3011-5012 and Fax: +55 44 3011-5046.

E-mail: cvnakamura@uem.br

Volpato, H. E-mail: helitovolpato2014@gmail.com

Miranda, N. E-mail: nathiellemiranda@gmail.com

Rodrigues, J. S. R. E-mail: jeanhsr@yahoo.com.br

Jacomini, A. P. E-mail: andreyjacomini@hotmail.com

Rosa, F. A. E-mail: farosa@uem.br

Sarragiotto, M. H. E-mail: mhsarragiotto@uem.br

Ueda-Nakamura, T. E-mail: tunakamura@uem.br

Silva S.O. E-mail: lautenschlager@uem.br

ABSTRACT

Leishmaniasis is a complex of diseases caused by protozoa species of the genus *Leishmania* sp. The current treatment of patients with leishmaniasis is very difficult, since the current drugs available demonstrate several adverse effects, and some cases of resistance. In this way, new biological active compounds are necessary for the treatment of patients infected with *Leishmania* sp. In previous studies, 4-[(2*E*)-*N'*-(2,2'-bithienyl-5-methylene)hydrazinecarbonyl]-6,7-dihydro-1-phenyl-1*H*-pyrazolo[3,4-*d*]pyridazin-7-one **(T6)** demonstrated a considerable selectivity in promastigote forms of *L. amazonensis*. Thus, our objective was to evaluate the involvement of oxidative stress as a mechanism of action of the compound in promastigotes of *L. amazonensis*, and thus to identify the type of cell death. Our results demonstrated that **T6** induces oxidative stress in the protozoan, being responsible for events that characterize cell death by apoptosis and necrosis. We can also verify the presence of autophagic vacuoles, which are induced by the parasite itself as an important way to promote cell survival and homeostasis.

KEYWORDS: leishmaniasis, *Leishmania* sp., thiophene, apoptosis, necrosis and oxidative stress.

INTRODUCTION

Leishmaniasis is a disease caused by more than 20 species of the protozoan *Leishmania* sp., being transmitted through the bite of females phlebotomines. Approximately 350 million people live in areas at risk of the disease, with 14 million people directly affected by leishmaniasis (PACE, 2014). Leishmaniasis can manifest itself in three main forms: cutaneous, mucocutaneous and visceral (or kala-azar) leishmaniasis. Cutaneous leishmaniasis is the most common form of the disease, being characterized by lesions on the skin. It is estimated that there will be 0.6 to 1 million new cases worldwide annually ("WHO | Leishmaniasis", 2017).

The treatment has been carried out basically through three drugs: pentavalent antimonials, amphotericin B and miltefosine. Unfortunately, current treatments have shown some limiting factors, such as long treatment time (BERMAN; HERWALDT, 1992), side effects (AKBARI; ORYAN; HATAM, 2017; IGBINEWEKA et al., 2012; MINODIER; PAROLA, 2007) and some cases of resistance in extensive treatments (DAS et al., 2011). Due to the limitations of current drugs, studies on the search for biologically active compounds natural or synthetic anti-*Leishmania* have been carried out in the search for the development of a new drug for the treatment of patients with leishmaniasis (GARCIA et al., 2016; VOLPATO et al., 2013).

Recently, a screening of the biological activity of new compounds derived from pyrazolo[3,4-d]pyridazin-7-one was carried out in promastigote forms of *L. amazonensis*. The results pointed out better activities of pyrazolo [3,4-*d]*-pyridazin-7-one-*N*-acylhydrazone-(bi)thiophene hybrids, such as for example 4-[(2*E*)-*N'*-(2,2'-bithienyl-5-methylene)hydrazinecarbonyl]-6,7-dihydro-1-phenyl-1*H*-pyrazolo[3,4-*d*]pyridazin-7-one (**T6**; Fig. 01). This compound showed an inhibitory concentration for 50% (IC$_{50}$) of the parasites of 10.79 μM, after 72 h of incubation. In mammalian cells, **T6** demonstrated a cytotoxic concentration for 50% (CC$_{50}$) of 114.33 μM, being more selective for the parasite (JACOMINI et al., 2016). The promising selectivity of **T6** in the parasite may be related to some peculiar cellular characteristics of *Leishmania* sp., such as the antioxidant system. Trypanothione reductase (TR) is a crucial enzyme in the redox system of these parasites, being absent in mammalian cells. Due to this exclusivity, TR has been the target of studies of chemotherapeutic agents against *Leishmania* sp. (BAIOCCO et al., 2013; LEROUX; KRAUTH-SIEGEL, 2016c). Through molecular docking analysis, an important affinity of the **T6** molecule has been revealed with some amino acid residues from the active site of the TR enzyme, which may lead to enzymatic inhibition (JACOMINI et al., 2016). Thus, the objective of the present study was to evaluate the in vitro action mechanism of **T6** in promastigotes of *L. amazonensis*, a species responsible

for cutaneous leishmaniasis. For this, several biochemical methodologies were developed for the study of oxidative stress and determine type of cell death.

MATERIALS AND METHODS

Chemistry

Antimycin A (AA); Camptothecin; Cyanide *m*-chlorophenylhydrazone (CCCP); 2',7'-dichlorofluorescin diacetate (H$_2$DCFDA); Digitonin; 2,2'-dinitro-5,5'-dithiobenzoic acid (DTNB); Diphenyl-1-pyrenylphosphine (DPPP); Folic Acid; Hemin; Monodansylcadaverine (MDC); *N*-acetyl-L-cysteine (NAC); Nile Red; Tetramethylrhodamine (TMRE) and Wortmannin (WTM) were obtained from Sigma-Aldrich. Amplex Red Hydrogen Peroxide/Peroxidase Assay Kit; APO-BrdU TUNEL Assay Kit with Alexa Fluor/488 Anti-BrdU (TUNEL); Fetal Bovine Serum (FBS); MitoSOX Red Mitochondrial Superoxide Kit; Propidium Iodide (IP) were purchased from Invitrogen. Annexin-V conjugated with Fluorescein Isothiocyanate (annexin-V/FITC) was obtained from Gibco BRL-Life Technologies. Brain Heart Infusion (BHI) was obtained from Difco. Dimethylsulfoxide (DMSO) was obtained from Synth. EnzChek Caspase-3 Assay Kit #1 Z-DEVD-AMC Substrate was obtained from Thermo Fisher Scientific. Hydrogen peroxide (H$_2$O$_2$) was obtained from Nuclear. All reagents obtained were of analytical grade.

Compound

The compound 4-[(2*E*)-*N'*-(2,2'-bithienyl-5-methylene)hydrazinecarbonyl]-6,7-dihydro-1-phenyl-1*H*-pyrazolo[3,4-*d*]pyridazin-7-one (**T6**) was synthesized as previously described (JACOMINI et al., 2016) and a stock solution diluted in dimethylsulfoxide (DMSO) was prepared. The concentration of DMSO did not exceed 0.1% (v/v).

Cell culture

Promastigote forms of *Leishmania amazonensis* (WHOM/BR/75/JOSEFA) were maintained in Warren medium (brain heart infusion, hemin and folic acid; pH 7.0) supplemented with 10% fetal bovine serum (FBS) and incubated at 26 °C.

Anti-amastigote assay

Peritoneal macrophages (5×10^5 cells/mL) in RPMI 1640 medium supplemented with 10% FBS were added in 24-wells plates containing round coverslips and incubated

for 2 h at 37 °C. After incubation, the medium was removed, added promastigotes of *L. amazonensis* (3.5×10^6 parasites/mL) and incubated for 4 h at 34 °C. Then, non-phagocytized parasites were removed, and the treatment was performed. For the treatment with **T6**, firstly the compound was diluted in RPMI 1640 medium obtaining different concentrations, and then added in the plate and incubated for 48 h at 37 °C. After treatment, coverslips with cells were fixed with methanol and stained with Giemsa. The 50% inhibitory concentration of parasites number (IC_{50}) was determined in comparison with untreated through the count of 200 macrophages under a light microscope.

Ultrastructural analysis

Promastigote forms (1×10^6 parasites/mL) were treated with 10 and 20 µM **T6** for 24 h. Then, the parasites were washed in PBS, fixed with 2.5% glutaraldehyde in 0.1 M cacodylate buffer at 4 °C. Then, the parasites were post-fixed in solution containing 1% osmium tetroxide, 0.8% potassium ferrocyanide and 10 mM calcium chloride in 0.1 M cacodylate buffer, dehydrated in increasing concentrations of acetone and embedded in EPON resin for 72 h at 60 °C. Ultrathin sections were performed, stained with uranyl acetate and lead citrate, and viewed in the samples electron microscope JEOL 1400 JM (TEM).

Elucidation of the mechanism of action-T6

In order to elucidate the mechanism of action, promastigotes (1×10^6 parasites/mL) were treated with IC_{50} and $2xIC_{50}$ (10 and 20 µM, respectively) of **T6** and then performed several biochemical methodologies. Together, in some experiments the pre-treatment of a group with the antioxidant *N*-acetyl-L-cysteine (200 µM; NAC) for 3 h was carried out in order to evaluate the possible involvement of ROS in some biochemical alterations. The experiments were analyzed in a microplate reader (Victor X3; PerkinElmer[®]), microplate spectrophotometer (BIO-TEK Power Wave XS) or flow cytometry (BD FACSCalibur) with software (BD CellQuest Pro).

Levels of reduced thiols

We decided to evaluate *in vitro* the levels of reduced thiols by means of the 2,2'-dinitro-5,5'-dithiobenzoic acid method (DTNB), an important technique to evaluate the action of TR (LAZARIN-BIDÓIA et al., 2013). For this, the parasites treated as described above were washed in PBS, resuspended in Tris-HCl buffer (100 mM; pH 2.5)

and lysed by sonication. The samples were then centrifuged, and the supernatant collected. Samples were added in 96-well plate, incubated with DTNB (1 mM) and performed reading at 412 nm. Hydrogen peroxide (H_2O_2; 4 mM) was used as a positive control.

ROS levels

Quantification of total ROS levels was performed by 2',7'-dichlorofluorescin diacetate (H_2DCFDA). For this, the parasites treated as described above were washed in PBS, resuspended in PBS containing H_2DCFDA (10 µM) and incubated for 45 min in the absence of light. Then the samples were added in a 96-well black plate and fluorescence measured (λex:488 nm and λem:530 nm). H_2O_2 (4 mM) was used as a positive control.

Hydrogen peroxide

Quantification of hydrogen peroxide (H_2O_2) was performed by Amplex Red Hydrogen Peroxide/Peroxidase Assay Kit. For this, the parasites treated as described above were washed in PBS, resuspended in PBS containing 5 mM succinate and processed according to the manufacture's manual. Then the samples were added in a 96-well black plate and fluorescence measured (λex:571 nm and λem:585 nm). H_2O_2 (4 mM) was used as a positive control.

Mitochondrial superoxide anions

Quantification of mitochondrial superoxide anions ($O_2^{\bullet-}$) was performed by MitoSOX Red Mitochondrial Superoxide Kit. For this, the parasites treated as described above were washed in Krebs-Henseleit buffer (KH; containing 15 mM $NaHCO_3$, 5 mM KCl, 120 mM NaCl, 0.7 mM Na_2HPO_4 and 1.5 mM NaH_2PO_4; pH 7.3) resuspended in PBS containing MitoSOX reagent (5 µM) and incubated for 20 min in the absence of light. Then the samples were washed and resuspended with KH buffer and added in a 96-well black plate and fluorescence reading performed (λex:510 nm and λem:580 nm). Antimycin A (AA; 10 µM) was used as a positive control.

Mitochondrial membrane potential

The mitochondrial membrane potential ($\Delta\Psi_m$) was evaluated by tetramethylrhodamine (TMRE). For this, the parasites treated as described above were washed in PBS, resuspended in PBS containing 25 nM TMRE and incubated for 30 min in the absence of light. Then the samples were washed and resuspended with PBS and added in a 96-well black plate and fluorescence reading performed (λex:540 nm and

λem:595 nm). Carbonyl cyanide *m*-chlorophenylhydrazone (CCCP; 100 µM) was used as a positive control.

Adenosine triphosphate

The intracellular level of adenosine triphosphate (ATP) was evaluated by CellTiter-Glo Luminescent Cell Viability Assay. For this, the parasites treated as described above were washed in PBS, and then the samples (50 µL) were added on a 96-well white plate containing CellTiter-Glo reagent (50 µL), incubated for 10 min and the luminance quantified. CCCP (100 µM) was used as a positive control.

Lipoperoxidation

The lipid peroxidation was evaluated by diphenyl-1-pyrenylphosphine (DPPP). For this, the parasites treated as described above were washed in PBS, resuspended in PBS containing 5 µM DPPP and incubated for 15 min in the absence of light. Then the samples were added in a 96-well black plate and fluorescence measured (λex:355 nm and λem:460 nm). H_2O_2 (4 mM) was used as a positive control.

Lipid droplets

Quantitation of accumulation of lipid inclusions was evaluated by Nile Red. For this, the parasites treated as described above were washed in PBS, resuspended in PBS containing 50 µM Nile Red and incubated for 30 min in the absence of light. Then the samples were added in a 96-well black plate and fluorescence measured (λex:385 nm and λem:535 nm). H_2O_2 (4 mM) was used as a positive control.

Externalization of phosphatidylserine

The externalization of phosphatidylserine residues (PS) was performed by annexin-V conjugated with fluorescein isothiocyanate (annexin-V/FITC). For this, the parasites treated as described above were washed in PBS, resuspended in binding buffer (containing 140 mM NaCl, 5 mM $CaCl_2$ and 10 mM HEPES-Na; pH 7.4) and incubated with annexin-V/FITC for 15 min in the absence of light. Then the samples were added in a 96-well black plate and fluorescence measured (λex:494 nm and λem:518 nm). Camptothecin (10 µM) was used as a positive control.

Active caspase-like

Quantification of active caspase-like was performed by EnzChek Caspase-3 Assay Kit #1 Z-DEVD-AMC Substrate. For this, the parasites treated as described above were

washed in PBS and incubated with Caspase-3 Assay Kit according to the manufacturer's instructions with some modifications. Then the samples were added in a 96-well black plate and fluorescence measured (λex:342 nm and λem:441 nm). In parallel, a group was preincubated with Ac-DEVD-CHO inhibitor (NICHOLSON et al., 1995) to confirm the fluorescence of the substrate. Camptothecin (10 µM) was used as a positive control.

DNA fragmentation

The analysis of DNA fragmentation was evaluated by APO-BrdU TUNEL Assay Kit with Alexa Fluor 488 Anti-BrdU (TUNEL kit). For this, the parasites treated as described above were washed in PBS, fixed with 4% paraformaldehyde and permeabilized with 0.2% Triton X-100 for 10 min. The samples were then incubated with TUNEL Kit with some modifications. After incubation, the samples were added in a 96-well black plate and fluorescence measured (λex:485 nm and λem:520 nm). Camptothecin (10 µM) was used as a positive control.

Cell cycle analysis

The cell cycle analysis was evaluated by permeabilization and labeling the cells with propidium iodide (PI). For this, the parasites treated as described above were washed in PBS, resuspended in ice-cold methanol (70% in PBS) and incubated at 4ºC for 2 h. For efficient permeabilization of methanol, the samples were homogenized every 30 min. After the permeabilization process, the samples were washed twice in PBS, resuspended in PBS containing PI (10 µg/mL) plus RNAse, incubated at 37°C for 45 min and performed reading 10,000 events. Taxol (10 µM) was used as a positive control.

Plasma membrane integrity

The evaluation of plasma membrane integrity was evaluated by PI. For this, the parasites treated as described above were washed in PBS, resuspended in PBS containing PI (0.2 µg/mL) and incubated for 5 min in the absence of light. Then the samples were added in a 96-well black plate and fluorescence measured (λex:535 nm and λem:617 nm). Digitonin (40 µM) was used as a positive control.

Autophagic vacuoles

The identification of autophagic vacuoles was evaluated by monodansylcadaverine (MDC). For this, the parasites treated as described above were washed in PBS, resuspended in PBS containing 0.05 mM MDC and incubated for 60 min in the absence of light. Then the samples were added in a 96-well black plate and

fluorescence measured (λex:335 nm and λem:518 nm). In parallel, a group was preincubated with wortmannin (WTM; 0.5 µM). WTM is described as a selective, potent and irreversible inhibitor of phosphatidylinositol 3-kinase (PI3 kinase), an enzyme related to the autophagic process (BLOMMAART et al., 1997). Old cultures of promastigotes (7-days) were used as positive control.

Statistical analysis

Data from all assays are expressed as mean and standard deviation ($\pm$ SD) of at least three independent experiments in duplicate or triplicate. The statistical analysis was performed using GraphPad Prism 5.0 (San Diego, CA, USA). The data were analyzed using one-way or two-way analysis of variance (ANOVA) and Bonferroni *post hoc* test was used to compare means. Values of $p \leq 0.05$ were considered statistically significant.

RESULTS

Anti-amastigote effect of T6

In this work it was possible to evaluate the effect of **T6**, a synthetic compound, on intracellular amastigote of *L. amazonensis*. An IC$_{50}$ of 19.31$\pm$4.24 µM of **T6,** after 48 h of treatment, was observed.

Ultrastructural effects of T6

Untreated parasites (Fig. 2-A) demonstrated common features, such as the presence of a nucleus, mitochondria and kinetoplast, a flagellar pocket containing only free flagellum and an elongated cell body. Promastigote forms treated with 10 µM of **T6** (Fig. 2 B-D) demonstrated ultrastructural changes, such as mitochondrial swelling, autophagic vacuoles, lipid bodies and concentric structures of membranes. Similar changes were observed in the parasites treated with 20 µM of **T6** (Fig. 2-E and F), however it was possible to verify an uncommon alteration, the presence of a mitochondria surrounded by an autophagic vacuole, giving a characteristic of mitochondrial macrophagy known as mitophagy.

T6 caused a decrease in the levels of reduced thiols

Our results demonstrated that 24 h treatment demonstrated a marked decrease in the levels of reduced thiols in **T6** treated parasites, with 53.62 and 62.21% of reduction compared to the untreated group at 10 and 20 µM of **T6**, respectively (Fig. 03 A).

Pretreatment with NAC did not protect the treated parasites at both concentrations. H_2O_2 was used as an inducer of oxidative stress, and caused a decrease of reduced thiols.

T6 induces increase of ROS

H_2DCFDA is a permeable marker used to measure levels of ROS, especially H_2O_2. It is based on the cleavage of the acetates groups by intracellular esterases, converting H_2DCFDA into the highly green-fluorescent compound 2', 7'-dichlorofluorescein (DCF). **T6** increased the levels of total ROS by 210.75 and 1,708.72%, respectively the treatment of 10 and 20 µM (Fig. 03 B). NAC reduced ROS levels only in the group treated with 20 µM, corresponding to 80.50%. H_2O_2 was used as a positive control and induced an increase ROS levels in parasites.

T6 induces increase of H_2O_2

The Amplex Red Kit is commonly used in the detection of H_2O_2 levels. It is a technique based on the reaction of Amplex Red reagents and horseradish peroxidase (HRP) with the H_2O_2 of the biological sample, producing red-fluorescent oxidation product, the resorufin. Treatment with **T6** showed an increase in H_2O_2 levels, corresponding to 506.78 and 1,063.86 %, respectively, the concentration of 10 and 20 µM, compared to the untreated group (Fig. 03 C). Pretreatment with NAC decreases the levels of hydrogen peroxide by 6.49% at the concentration of 20 µM of **T6**. H_2O_2 was used as a positive control and caused an increase of ROS levels.

T6 induces increased mitochondrial $O_2^{\bullet-}$

MitoSOX Red is a permeable reagent used to measure levels of mitochondrial $O_2^{\bullet-}$. It is based on oxidation in the presence of $O_2^{\bullet-}$, forming a product that binds to nucleic acids and emits red-fluorescence. **T6** caused increase of mitochondrial $O_2^{\bullet-}$ in the parasites treated with the two concentrations tested. The concentration of 10 µM caused an increase of 506.78%, and at the concentration of 20 µM there was an increase of 1,063.86% (Fig. 03 D). In pre-treatment with NAC, there was a decrease only in the group treated with 20 µM. AA, an electron transfer inhibitor of the complex III of the electron transport chain in the mitochondria, was used as a positive control, and induced an increase in mitochondrial $O_2^{\bullet-}$ levels.

T6 did not cause change in ΔΨm

TMRE is a fluorescent dye permeable to cells and it is easily sequestered by mitochondria due to its chemical characteristics. Thus, cells with the ΔΨm viable have a

higher fluorescence, compared to cells with a mitochondrial depolarization. Parasites treated with **T6** for 24 h did not cause change in $\Delta\Psi$m (Fig. 04 A). CCCP, known as a strong decoupling of oxidative phosphorylation in mitochondria, was used as a positive control and caused a decrease in $\Delta\Psi$m of the parasite.

T6 induces an increase in intracellular ATP levels

CellTiter-Glo Luminescent is a reagent used to determine cell viability through the quantification of ATP. The method is based on the reaction of luciferin with luciferase in the presence of ATP, producing high luminance. There was no decrease in intracellular ATP levels in both treatments for 24 h with **T6**, demonstrating that mitochondrion is in normal activity. Interestingly, the treatment of 10 µM caused a 40.31% increase in ATP levels compared to the untreated group (Fig. 04 B). At the same concentration of the compound, the NAC decreases the levels of ATP. CCCP was used as a positive control, demonstrating a considerable decrease in ATP levels.

T6 causes lipid peroxidation

The DPPP is a marker used to detect a lipid peroxidation product. DPPP is a non-fluorescent probe to be oxidized to a fluorescent product in the presence of hydroperoxide. **T6** at concentrations of 10 and 20 µM caused an increase in the lipoperoxidation process (637.37 and 2,221.37%, respectively; Fig. 05 A). Pretreatment with NAC caused a protection in the highest concentration of **T6**. H_2O_2 induced an increase in lipid peroxidation compared to the untreated control.

T6 caused an increase in lipid bodies

To verify a possible alteration in the formation of lipid bodies, we performed the labeling of the parasites with Nile Red, a dye with low fluorescence that has great affinity mainly with neutral lipids, and thus emits high red-fluorescence. We verified after the treatment for 24 h with **T6** in the two concentrations tested, 10 and 20 µM, a significant increase of 140.29 and 244.10% respectively (Fig. 05 B). The levels of lipid bodies after pretreatment with NAC were significantly reduced at both concentrations, demonstrating the involvement of oxidative stress. H_2O_2 was used as a positive control, which induced an increase of lipid bodies, and reduced in the presence of NAC.

T6 induces externalization of PS

A main apoptotic alteration is the externalization of the phospholipid PS in the external leaflet of the plasma membrane, a characteristic present also in protozoan

Trypanosomatids. For this, we use a PS-specific marker: annexin-V/FITC. During PS externalization, annexin-V/FITC binds to the phospholipid, and thus emits high green-fluorescence. Viable cells emit low fluorescence because PS localizes in the inner phase of the cell membrane. **T6** treatment was performed for 3 h in order to verify the onset of the apoptosis process, in order to verify the initial pathway of the protozoan cell death. The **T6** caused an increase in PS externalization at concentrations of 10 and 20 μM (122.96 and 303.79%, respectively; Fig. 06 A). Pretreatment with NAC was possible to decrease by 17.44 and 12.40%, respectively. This result demonstrates a direct involvement of ROS in the onset of apoptosis type cell death since the antioxidant treatment prevented it significantly.

T6 induces caspase-like activation

The EnzChek Caspase-3 Kit is a method that relies on the ability of the weakly fluorescent substrate Z-DEVD-AMC to bind to caspase-3 and produce a highly blue-fluorescent product after proteolytic cleavage. The kit can detect activity of other caspases having affinity to the substrate, such as caspase-7. After treatment for 24 h, it was possible to verify an increase in caspase 3/7-like activation at concentrations of 10 and 20 μM (121.038% and 298.41% respectively) of **T6** (Fig. 06 B). It was possible to verify a decrease in fluorescence in the group treated with 20 μM in the presence in the Ac-DEVD-CHO inhibitor. As positive control, an apoptosis inducer was used, the camptothecin (SEN et al., 2004), which caused an increase in fluorescence and the same treatment in the presence of the Ac-DEVD-CHO inhibitor, reduced 19.91%.

T6 induces DNA fragmentation

The method by TUNEL is based on the incorporation of the BrdUTP into exposed 3'hydroxyl ends due to cleavage process. After incorporation, BrdUTP binds to the anti-BrdU conjugated with Alexa Fluor 488 dye and emits green-fluorescence. There was a significant increase in DNA fragmentation in **T6**-treated parasites compared to the untreated group, concentrations of 10 and 20 μM showed an increase of 552.20 and 1,202.69%, respectively (Fig. 06 C). In the presence of the antioxidant NAC, the same treatments demonstrated a reduction of more than 50% in both concentrations, demonstrating an involvement of ROS in the process of DNA fragmentation, culminating in apoptosis cell death for apoptosis-like. Camptothecin was used as an inducer of apoptosis, and demonstrated significant fragmentation of the parasite DNA.

T6 alters cell cycle

The cell cycle is an indispensable mechanism for the survival of organisms, unicellular or multicellular. Thus, we decided to evaluate the possible effect of **T6** on the cell cycle of promastigotes of *L. amazonensis*. Only significant change was observed in parasites treated with 20 µM of the compound. There were alterations in the Sub-G0 (17.41%), S (13.55%) and G2/M (22.61% increase) in relation to the untreated control (Table 01). Taxol was used as a positive control and caused changes in the G0/G1 and G2/M compared to the untreated group**.**

T6 induces necrosis and autophagy

Alteration in plasma membrane integrity is one of the main features of necrotic cell death. Propidium iodide is a marker that is impermeable to plasma membrane, and has been screened for possible change in plasma membrane permeability. After treatment with the compound on promastigote forms, we found a significant change only at the concentration of 20 µM (Fig. 07 A). Pretreatment with NAC significantly reduced plasma membrane damage. Digitonin, a potent detergent, demonstrated significant damage to the permeability of the parasite's plasma membrane.

To analyze these possible autophagic events, promastigote forms treated for 24 h with **T6** were labeled with MDC (BIEDERBICK; KERN; ELSASSER, 1995; SCARIOT et al., 2017). The two concentrations induced the formation of autophagic vacuoles, corresponding to 789.85 and 609.68% respectively at 10 and 20 µM of **T6** (Fig. 07 B). In the presence of WTM, it was possible to verify a significant inhibition in the formation of autophagic vacuoles in both treatments with **T6**. As positive control, parasites were used with 7-days of culture, and an increase of fluorescence was observed, and the same in the presence of WTM there was a 37.10% decrease in the formation of autophagic vacuoles.

DISCUSSION

Analysis of the activity against the amastigote form of the parasite, found in the vertebrate host, is very important. In view of our results, we observed a promising activity of **T6** in the intracellular amastigote forms of *L. amazonensis*, collaborating with the results obtained previously against the promastigote forms (JACOMINI et al., 2016).

Elucidation of the mechanism of action is of great importance in the studies of biological active compounds (MIRANDA et al., 2017; VOLPATO et al., 2013). In this way we decided to evaluate the changes in the parasite treated with synthetic compound **T6**. These parasites have specific characteristics and are absent in the mammalian cells, such as the presence of a single mitochondria and the kinetoplast (FIDALGO; GILLE,

2011; WILKINSON; KELLY, 2009). We verified through MET several ultrastructural changes, such as mitochondrial swelling, autophagic vacuoles, lipid bodies and concentric structures of membranes. An interesting change in the parasites treated with **T6** was the presence of autophagic vacuole containing part of the mitochondria. This change, together with the presence of other autophagic vacuoles, could suggest two hypotheses: (*i*) **T6** induces cell death by autophagy (RODRIGUES et al., 2014; SCARIOT et al., 2017), or (*ii*) the parasite induces autophagy with the aim of reducing the damage caused by the compound, known as the mechanism of cytoprotection, maintaining cellular homeostasis (CHANDRIKA et al., 2015; HE; KLIONSKY, 2009; KROEMER; LEVINE, 2008). Through the results obtained by MET, we decided to verify a possible involvement of the autophagy in the survival of the parasite, as well as other types of cellular death: apoptosis and necrosis.

The uncontrolled increase in ROS is evidence of possible oxidative stress (BIRBEN et al., 2012; OTT et al., 2007) and contributes to the process the various types of cell death. Thus, we decided to evaluate the antioxidant system of *L. amazonensis*. It is described that protozoa of the family *Trypanosomatidae* have specific antioxidant system, absent in mammalian cells, known as trypanothione/trypanothione reductase (TS_2/TR) system (LEROUX; KRAUTH-SIEGEL, 2016b). The TS_2/TR system is one of the main targets of studies of bioactive molecules, since it demonstrates selectivity for the parasites (LAZARIN-BIDÓIA et al., 2013; LEROUX; KRAUTH-SIEGEL, 2016c; MIRANDA et al., 2017). By means of the DTNB assay, it was possible to verify a marked decrease in the levels of reduced thiols in the parasites treated with **T6**, demonstrating a possible induction of oxidative stress. In addition, through the labeling with Nile Red, we observed an increase of lipid droplets in the cytoplasm of parasites treated with **T6**. This increase in lipid bodies is due to changes in the phospholipid content caused by oxidative stress (Godinho et al., 2013; Lee et al., 2013; Volpato et al., 2015). The NAC was able to reduce the levels of lipid inclusions, proving the involvement of oxidative stress in causing increase of the lipid bodies in the parasite.

Apoptosis, a programmed cell death, is characterized by morphological and biochemical events. Exposure of phosphatidylserine (PS) to the outer leaflet of the plasma membrane is evidence of apoptosis (GALLUZZI et al., 2012), and annexin V/FITC is commonly used in the detection of this apoptotic event. We verified that **T6** induced an increase in exposure of PS residues significantly at both concentrations tested. Other important apoptotic features are DNA fragmentation and activation of caspases (GALLUZZI et al., 2012; MIRANDA et al., 2017). Our results demonstrated that **T6** caused activation of caspase 3/7-like (or metacaspases) and DNA fragmentation at both

concentrations (GONZALEZ et al., 2007). Interestingly, pre-treatment with NAC, a potent antioxidant (SHAHRIPOUR et al., 2014), significantly reduced apoptotic events (PS exposure and DNA fragmentation). This may demonstrate that apoptosis events may be being induced due to damage caused by ROS (REDZA-DUTORDOIR; AVERILL-BATES, 2016). To evaluate the involvement of ROS in the activation of apoptosis (MIRANDA et al., 2017; REDZA-DUTORDOIR; AVERILL-BATES, 2016), we decided to quantify the levels of ROS in the parasites treated with **T6**. H_2DCFDA, Amplex Red Kit and MitoSOX are important markers of ROS. Compared to controls, **T6** significantly induced the production of H_2O_2 (H_2DCFDA and Amplex Red Kit) and mitochondrial superoxide (MitoSOX). These results confirm the involvement of ROS in the events of cell death by apoptosis. High ROS production can cause strong cell damage due to its reactive capacity with biomolecules: proteins, lipids and nucleic acids (OTT et al., 2007; ROY et al., 2008). As previously reported, **T6** induced DNA fragmentation, and there was reduction of this alteration due to pretreatment with NAC. Thus, we decided to evaluate the effect of **T6** on other biomolecules, the lipids of membranes. Through the DPPP assay, we found an increase in lipid peroxidation in parasites treated with the synthetic compound. Pre-treatment with NAC significantly reduced lipid peroxidation at the highest concentration of **T6**, confirming the involvement of ROS in the oxidation of biomolecules (DAS et al., 2008; KATHURIA et al., 2014).

It is described that apoptosis is a differentiated form of cell death requiring energy (ATP), and has been related to activation of caspase-3 and DNA fragmentation (ZAMARAEVA et al., 2005). Thus, we decided in this work to perform the measurement of the levels of cytosolic ATP of the parasites treated with **T6**. We found that **T6** induced a significant increase in intracellular ATP levels only at the concentration of 10 µM. At the 20 µM concentration there was no change in the levels, remaining constant in relation to the control. These results point to the need for energy to induce cell death by apoptosis, as we have verified that the compound induced caspase activation and DNA fragmentation, both characteristics related to the increase of ATP levels (KASS et al., 1996; SEN et al., 2006; ZAMARAEVA et al., 2005). The potential of the mitochondrial membrane is of fundamental importance for the production of ATP in the cells. Thus, we decided to evaluate the mitochondrial membrane potential of the parasites treated with **T6**, because we showed that the compound induced an increase in cytosolic ATP. For this, we used the marker TMRE, commonly used to evaluate mitochondrial membrane potential. Through the obtained results, we verified that **T6** did not provoke changes in mitochondrial membrane potential. This result collaborates with the ATP quantification assay, as we verified that ATP levels were not compromised.

The cell cycle is of immense importance to cells, including to unicellular organisms such as protozoa, and disturbances in the division may compromise the survival of the parasite. We decided, by flow cytometry, to analyze the various phases of the cell cycle of promastigote forms treated with **T6**. The results showed significant changes in the highest concentration tested (20 μM). There was a decrease in S phase cells and an increase in the G2/M phase population. It is described that the sub-G0 phase is represented by cells with fragmented DNA, and our results indicate an increase in the percentage of cells at this stage, collaborating with the results obtained by TUNEL technique.

Alteration of plasma membrane permeability and the presence of autophagic vacuoles are the main evidences of cell death due to necrosis and autophagy, respectively (GLICK et al., 2010; THORNTON; HAGBERG, 2014). In this way, we verified biochemically these two characteristics in the parasites treated with **T6**. Our results demonstrated a change in permeability after treatment with **T6** for 24 h. This result, together with the results of PS externalization, DNA fragmentation, caspase-like demonstrates that **T6** induces cell death by apoptosis, and subsequently death by necrosis. To evaluate the presence of autophagic vacuoles, we performed the marking of parasites with MDC. **T6** induced an increase of autophagic vacuoles at both concentrations tested, after 24 h of treatment. Similar result was observed by ultrastructural analysis in MET. Interestingly, the concentration of 20 μM of **T6** demonstrated a lower level of autophagic vacuoles. This difference may highlight the hypothesis cited at the beginning: (*ii*) parasite induce autophagy to reduce the damage caused by treatment with **T6**, because most of the assays at the concentration of 20 μM caused an increase in cellular damage. These damages could be considered irreversible for the autophagy cytoprotection process (CHANDRIKA et al., 2015; HE; KLIONSKY, 2009; KROEMER; LEVINE, 2008).

CONCLUSION

T6 has shown promising activity in *L. amazonensis*. We verified that the activity of the compound in the parasite is due to alteration in the cellular homeostasis, causing irreversible damages that culminate in the death of the protozoan: apoptosis followed by necrosis. These results indicate **T6** is an interesting compound in the development of new drugs for the treatment of patients with leishmaniasis.

Acknowledgments

References

AKBARI, M.; ORYAN, A.; HATAM, G. Application of nanotechnology in treatment of leishmaniasis: A Review. **Acta Tropica**, v. 172, p. 86–90, ago. 2017.

BAIOCCO, P. et al. Inhibition of *Leishmania infantum* trypanothione reductase by azole-based compounds: a comparative analysis with its physiological substrate by X-ray crystallography. **ChemMedChem.**, v. 8, n. 7, p. 1175–1183, jul. 2013.

BERMAN, J. D.; HERWALDT, B. L. Recommendations for treating leishmaniasis with sodium stibogluconate (Pentostam) and review of pertinent clinical studies. **The American Journal of Tropical Medicine and Hygiene.**, v. 46, n. 3, p. 296–306, 1 mar. 1992.

BIEDERBICK, A.; KERN, H. F.; ELSASSER, H. P. Monodansylcadaverine (MDC) is a specific in vivo marker for autophagic vacuoles. **European Journal of Cell Biology.**, v. 66, n. 1, p. 3–14, jan. 1995.

BIRBEN, E. et al. Oxidative stress and antioxidant defense. **World Allergy Organization Journal**, v. 5, n. January, p. 9–19, 2012.

BLOMMAART, E. F. C. et al. The phosphatidylinositol 3-kinase inhibitors wortmannin and LY 294002 inhibit autophagy in isolated rat hepatocytes. **European Journal of Biochemistry**, v. 246, p. 240–246, 1997.

CHANDRIKA, B. B. et al. Endoplasmic reticulum stress-induced autophagy provides cytoprotection from chemical hypoxia and oxidant injury and ameliorates renal ischemia-reperfusion injury. **PloS ONE**, v. 10, n. 10, p. e0140025, 2015.

DAS, R. et al. Reactive oxygen species and imbalance of calcium homeostasis contributes to curcumin induced programmed cell death in *Leishmania donovani*. **Apoptosis**, v. 13, 2008.

DAS, S. et al. Miltefosine loaded albumin microparticles for treatment of visceral leishmaniasis: formulation development and in vitro evaluation. **Polymers for Advanced Technologies**, v. 22, n. 1, p. 172–179, 1 jan. 2011.

FIDALGO, L. M.; GILLE, L. Mitochondria and trypanosomatids: Targets and drugs. **Pharmaceutical Research**, v. 28, n. 11, p. 2758–2770, 2011.

GALLUZZI, L. et al. Molecular definitions of cell death subroutines: recommendations of the Nomenclature Committee on Cell Death 2012. **Cell death and Differentiation**, v. 19, n. 1, p. 107–120, 15 jan. 2012.

GARCIA, F. P. et al. A3K2A3-induced apoptotic cell death of *Leishmania amazonensis* occurs through caspase- and ATP-dependent mitochondrial dysfunction. **Apoptosis**, p. 1–15, 2016.

GLICK, D.; BARTH, S.; MACLEOD, K. F. Autophagy: cellular and molecular mechanisms. **The Journal of Pathology**, v. 221, n. 1, p. 3–12, maio 2010.

GODINHO, J. L. P. et al. A novel alkyl phosphocholine-dinitroaniline hybrid molecule exhibits biological activity in vitro against *Leishmania amazonensis*. **Experimental Parasitology**, v. 135, n. 1, p. 153–165, set. 2013.

GONZALEZ, I. J. et al. *Leishmania major* metacaspase can replace yeast metacaspase in programmed cell death and has arginine-specific cysteine peptidase activity. **The International Journal for Parasitology**, v. 37, 2007.

HE, C.; KLIONSKY, D. J. Regulation mechanisms and signaling pathways of autophagy. **Annual Review of Genetics**, v. 43, n. 1, p. 67–93, dez. 2009.

IGBINEWEKA, O. et al. Evaluating the efficacy of topical silver nitrate and intramuscular antimonial drugs in the treatment of cutaneous leishmaniasis in Sokoto, Nigeria. **African Journal of Clinical and Experimental Microbiology**, v. 13, n. 2, p. 90–97, 12 mar. 2012.

JACOMINI, A. P. et al. Synthesis and evaluation against *Leishmania amazonensis* of novel pyrazolo[3,4-d]pyridazinone-N-acylhydrazone-(bi)thiophene hybrids. **European Journal of Medicinal Chemistry**, v. 124, 2016.

KASS, G. E. et al. Chromatin condensation during apoptosis requires ATP. **The**

Biochemical Journal, v. 318 (Pt 3), n. Pt 3, p. 749–52, 15 set. 1996.

KATHURIA, M. et al. Induction of mitochondrial dysfunction and oxidative stress in *Leishmania donovani* by orally active clerodane diterpene. **Antimicrobial Agents and Chemotherapy**, v. 58, n. 10, p. 5916–5928, 2014.

KROEMER, G.; LEVINE, B. Autophagic cell death: the story of a misnomer. **Nature Reviews Molecular Cell Biology**, v. 9, n. 12, p. 1004–1010, 30 dez. 2008.

LAZARIN-BIDÓIA, D. et al. Further evidence of the trypanocidal action of eupomatenoid-5: Confirmation of involvement of reactive oxygen species and mitochondria owing to a reduction in trypanothione reductase activity. **Free Radical Biology and Medicine**, v. 60, p. 17–28, 2013.

LEE, S. J., ZHANG, J., CHOI, A. M. K., KIM, H. P. Mitochondrial dysfunction induces formation of lipid droplets as a generalized response to stress. **Oxidative Medicine and Cellular Longevity**, v. 327, p. 1–10, 2013.

LEROUX, A. E.; KRAUTH-SIEGEL, R. L. Thiol redox biology of trypanosomatids and potential targets for chemotherapy. **Molecular and Biochemical Parasitology**, v. 206, n. 1, p. 67–74, 2016a.

MINODIER, P.; PAROLA, P. Cutaneous leishmaniasis treatment. **Travel Medicine and Infectious Disease**, v. 5, n. 3, p. 150–158, maio 2007.

MIRANDA, N. et al. The photodynamic action of pheophorbide *a* induces cell death through oxidative stress in *Leishmania amazonensis*. **Journal of Photochemistry and Photobiology B: Biology**, v. 174, 2017.

NICHOLSON, D. W. et al. Identification and inhibition of the ICE/CED-3 protease necessary for mammalian apoptosis. **Nature**, v. 376, n. 6535, p. 37–43, 6 jul. 1995.

OTT, M. et al. Mitochondria, oxidative stress and cell death. **Apoptosis**, v. 12, n. 5, p. 913–922, 2007.

PACE, D. Leishmaniasis. **Journal of Infection**, v. 69, p. S10–S18, nov. 2014.

REDZA-DUTORDOIR, M.; AVERILL-BATES, D. A. Activation of apoptosis signalling pathways by reactive oxygen species. **Biochimica et Biophysica Acta (BBA) - Molecular Cell Research**, v. 1863, n. 12, p. 2977–2992, 2016.

RODRIGUES, J. H. DA S. et al. A quinoxaline derivative as a potent chemotherapeutic agent, alone or in combination with benznidazole, against *Trypanosoma cruzi*. **PLoS ONE**, v. 9, n. 1, p. e85706, 17 jan. 2014.

ROY, A. et al. Mitochondria dependent ROS-mediated programmed cell death (PCD) induced by 3,3'-Diindolylmethane (DIM) through Inhibition of FoF1-ATP synthase in unicellular protozoan parasite *Leishmania donovani*. **Molecular Pharmacology**, v. 74, 2008.

SCARIOT, D. B. et al. Induction of early autophagic process on *Leishmania amazonensis* by synergistic effect of Miltefosine and innovative semi-synthetic thiosemicarbazone. **Frontiers in Microbiology**, v. 8, p. 255, 21, 2017.

SEN, N. et al. Camptothecin-induced imbalance in intracellular cation homeostasis regulates programmed cell death in unicellular hemoflagellate Leishmania donovani. **Journal of Biological Chemistry**, v. 279, 2004.

SEN, N. et al. *Leishmania donovani*: intracellular ATP level regulates apoptosis-like death in luteolin induced dyskinetoplastid cells. **Experimental Parasitology**, v. 114, 2006.

SHAHRIPOUR, R. B.; HARRIGAN, M. R.; ALEXANDROV, A. V. N -acetylcysteine (NAC) in neurological disorders : mechanisms of action and therapeutic opportunities. **Brain and Behaviour**, v. 4, p. 108–122, 2014.

THORNTON, C.; HAGBERG, H. Role of mitochondria in apoptotic and necroptotic cell death in the developing brain. **Clinica Chimica Acta**, v. 451, p. 35–38, 2014.

VOLPATO, H. et al. The Effects of N-butyl-1-(4-dimethylamino)phenyl-1,2,3,4-tetrahydro-β-carboline-3-carboxamide against *Leishmania amazonensis* are mediated by mitochondrial dysfunction. **Evidence-based complementary and alternative medicine :**

eCAM, v. 2013, p. 874367, 2013.

VOLPATO, H. et al. Mitochondrial dysfunction induced by N-tetrahydro-β-carboline-3-carboxamide is required for cell death of *Trypanosoma cruzi*. **PLoS ONE**, v. 10, p. 1–11, 2015.

WHO | Leishmaniasis. Avaliable in: <http://www.who.int/mediacentre/factsheets/fs375/en/>. In: 24 jul. 2017.

WILKINSON, S. R.; KELLY, J. M. Trypanocidal drugs: mechanisms, resistance and new targets. **Expert Reviews in Molecular Medicine**, v. 11, p. e31, 29 out. 2009.

ZAMARAEVA, M. V et al. Cells die with increased cytosolic ATP during apoptosis: a bioluminescence study with intracellular luciferase. **Cell Death and Differentiation**, v. 12, n. 11, p. 1390–7, 2005.

TABLE AND FIGURE
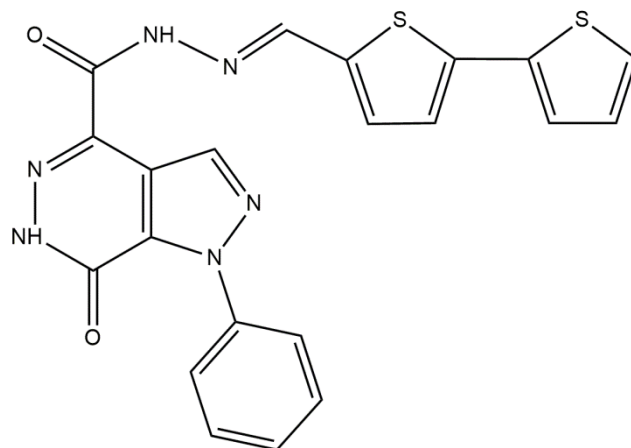
Figure 01. Chemical structure of synthetic compound 4-[(2*E*)-*N*'-(2,2'-bithienyl-5-methylene)hydrazinecarbonyl]-6,7-dihydro-1-phenyl-1*H*-pyrazolo[3,4-*d*]pyridazin-7-one (**T6**). Chemical formula: $C_{21}H_{15}N_6O_2S_2$ and molecular weight: 447.06.
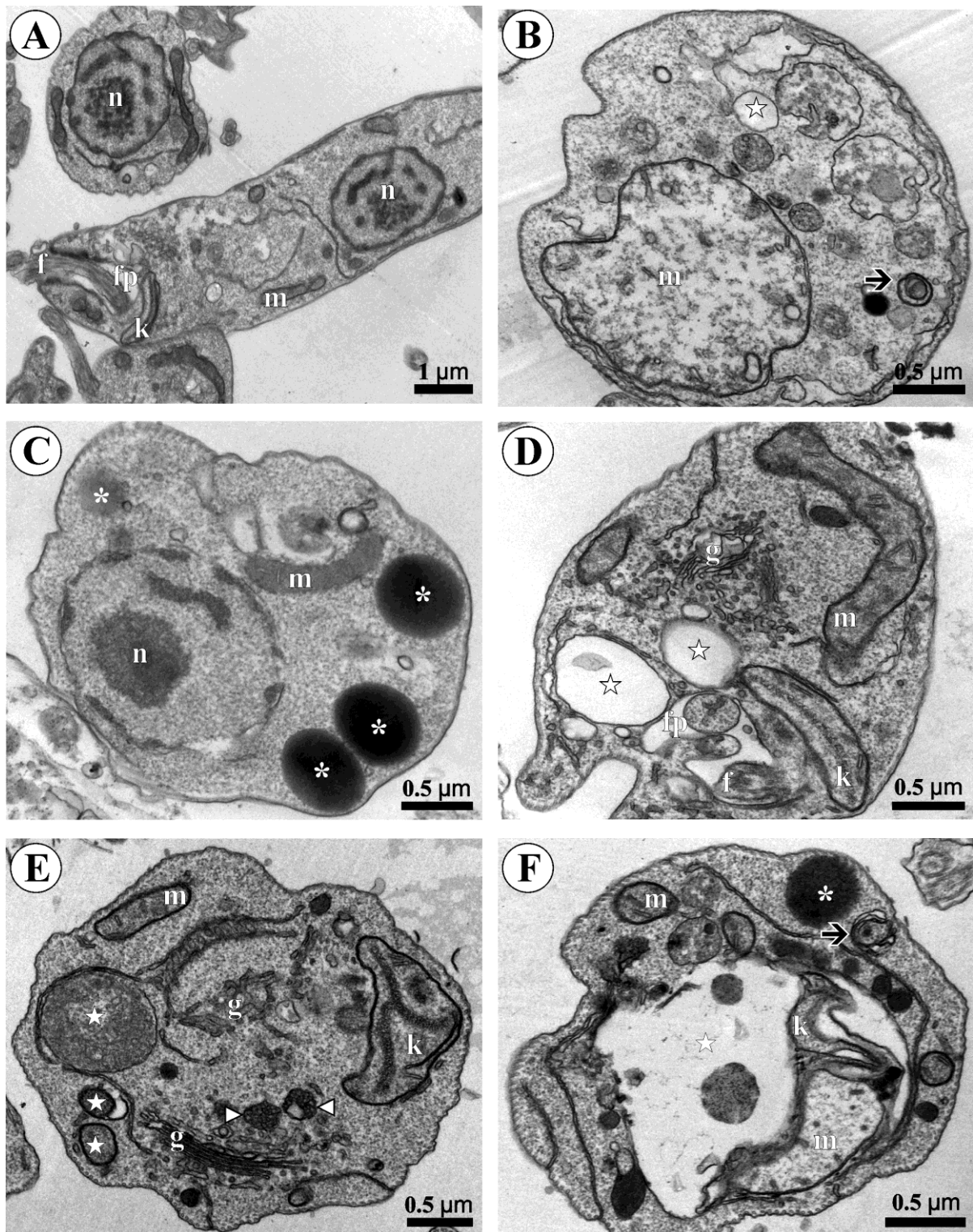
Figure 02. Ultrastructural analysis by transmission electron microscopy in *Leishmania amazonensis* **promastigote forms treated with synthetic compound T6 for 24 h. (A)** Untreated, **(B-D)** treated with 10 µM and **(E and F)** treated with 20 µM. (n) nucleus, (m) Mitochondria, (k) kinetoplast, (fp) flagellar pocket, (f) flagellum, (g) Golgi complex (white star) autophagic vacuoles, (white asterisk) lipid inclusion, (black arrow) membrane concentric structure and (white triangle) multi-vesicular bodies.
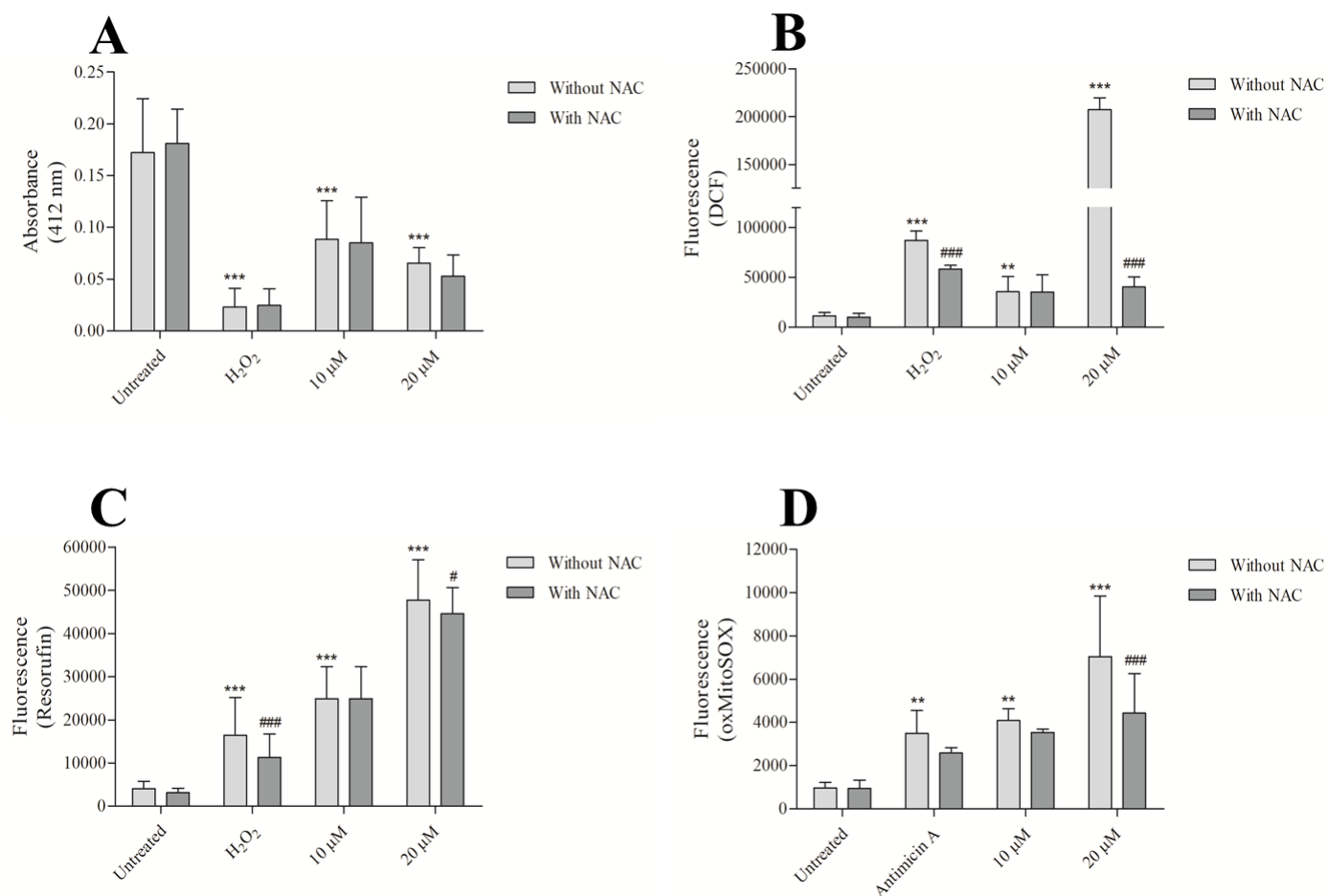
Figure 03. Elucidation of the mechanism of action in promastigote forms of *Leishmania amazonensis* **treated with T6 synthetic compound. (A)** Quantification of thiols levels, **(B)** detection of ROS levels, **(C)** detection of the levels of hydrogen peroxide and **(D)** detection of mitochondrial superoxide levels. The pretreatment was carried out with a group of *N*-acetylcysteine antioxidant (NAC; 20 µM). The data are expressed as mean fluorescence ± SD. **(*)** significantly different from untreated group without NAC ($^{**}p \leq 0.01$ and $^{***}p \leq 0.001$). **(#)** significantly different from the same treatment without NAC ($^{#}p \leq 0.05$ and $^{###}p \leq 0.001$). Data from all assays are expressed as mean and standard deviation (± SD) of at least three independent experiments in triplicate.
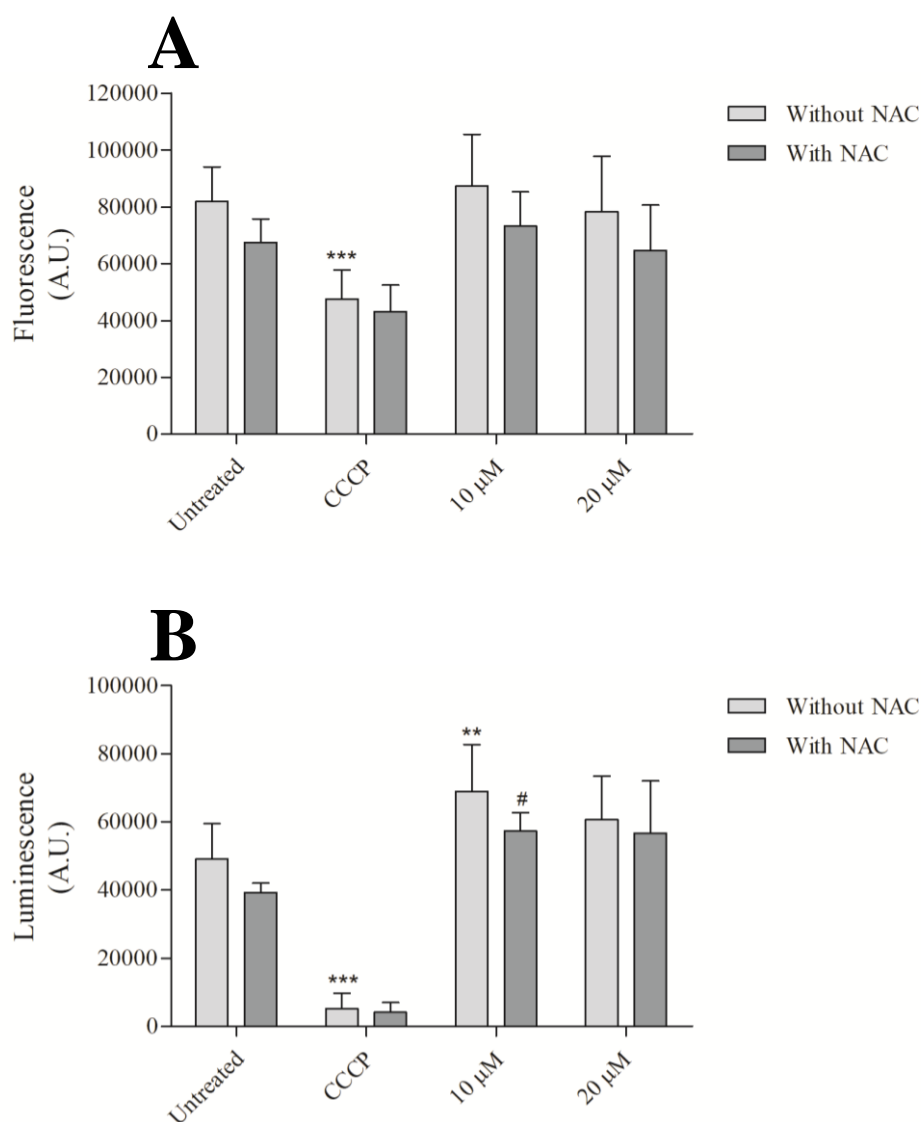
Figure 04. Elucidation of the mechanism of action in promastigote forms of *Leishmania amazonensis* treated with T6 synthetic compound. **(A)** Evaluation of the mitochondrial membrane potential and **(B)** quantification of intracellular ATP. The pretreatment was carried out with a group of *N*-acetylcysteine antioxidant (NAC; 20 µM). The data are expressed as mean fluorescence ± SD. **(*)** significantly different from untreated group without NAC ($^{**}p \leq 0.01$ and $^{***}p \leq 0.001$). **(#)** significantly different from the same treatment without NAC ($^{#}p \leq 0.05$). Data from all assays are expressed as mean and standard deviation (± SD) of at least three independent experiments in triplicate.
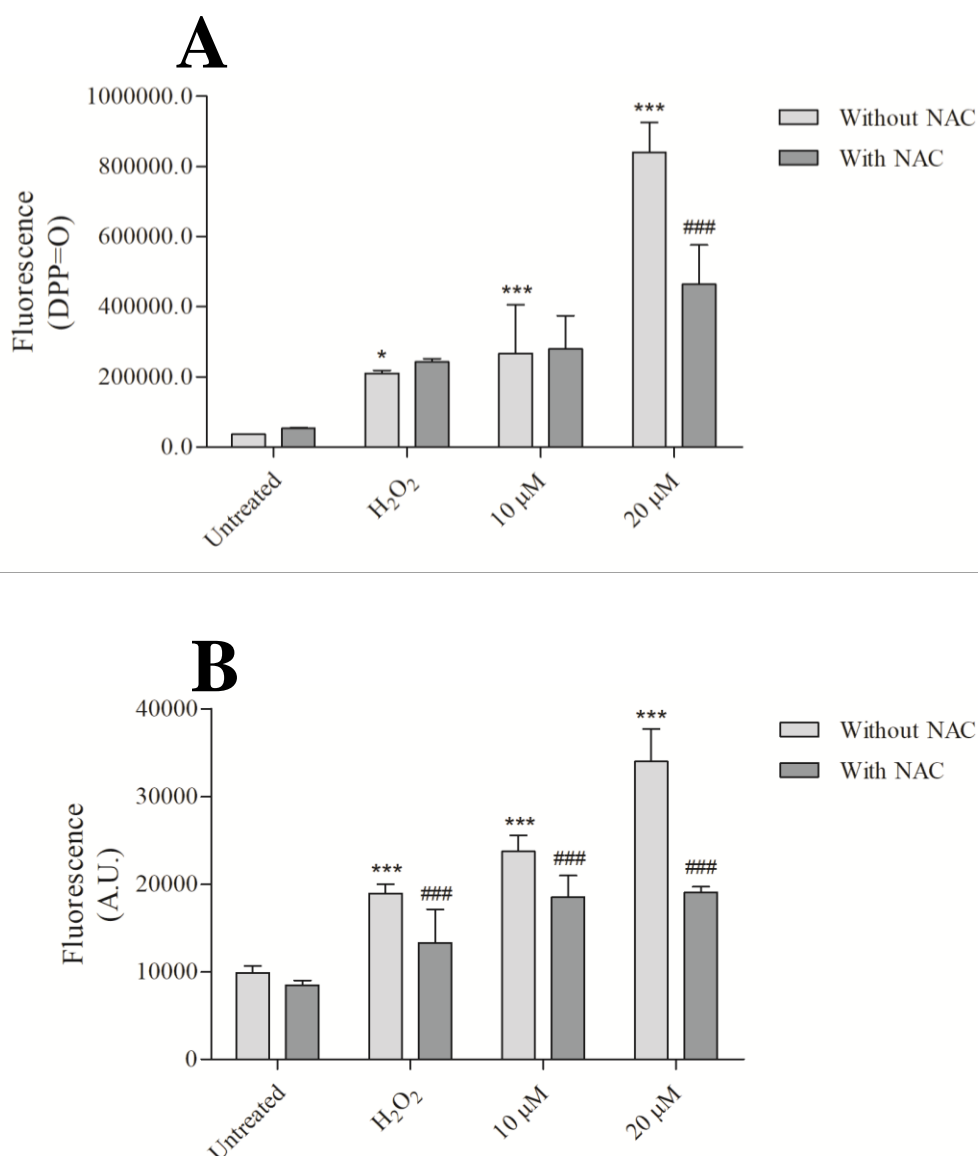
A

B

Figure 05. Elucidation of the mechanism of action in promastigote forms of *Leishmania amazonensis* **treated with T6 synthetic compound. (A)** Detection of lipid peroxidation and (B) detection of lipid bodies levels. The pretreatment was carried out with a group of *N*-acetylcysteine antioxidant (NAC; 20 µM). The data are expressed as mean fluorescence ± SD. **(*)** significantly different from untreated group without NAC ($^{*}p \leq 0.05$ and $^{***}p \leq 0.001$). **(#)** significantly different from the same treatment without NAC ($^{\#\#\#}p \leq 0.001$). Data from all assays are expressed as mean and standard deviation (± SD) of at least three independent experiments in triplicate.
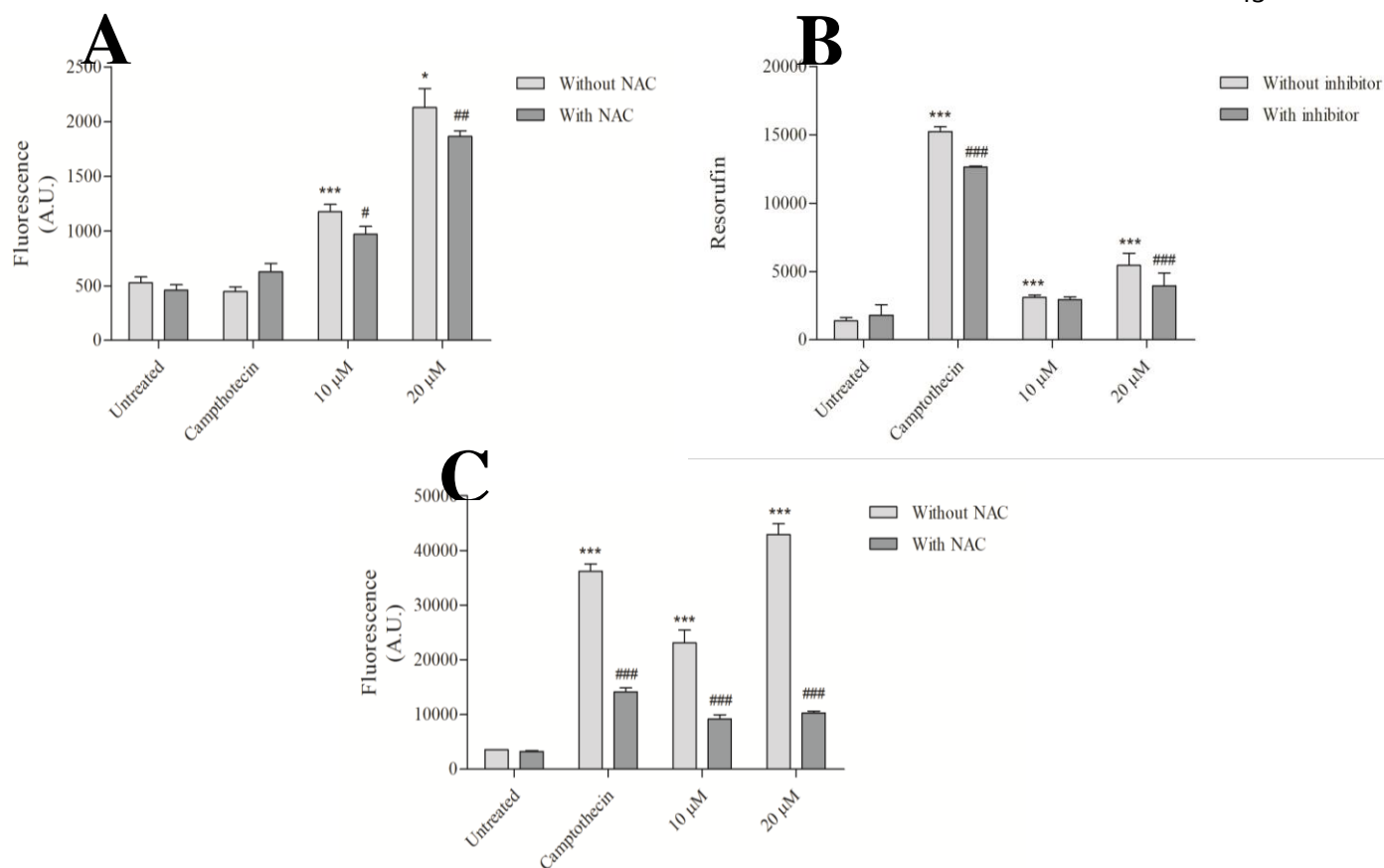
Figure 06. Elucidation of the mechanism of action in promastigote forms of *Leishmania amazonensis* treated with T6 synthetic compound. (A) Detection of phosphatidylserine, **(B)** quantification of active caspases-like and **(C)** detection of DNA fragmentation. The pretreatment was carried out with a group of *N*-acetylcysteine antioxidant (NAC; 20 μM) or the Ac-DEVD-CHO inhibitor. The data are expressed as mean fluorescence ± SD. (*****) significantly different from untreated group without NAC or inhibitor ($^{*}p \leq 0.05$ and $^{***}p \leq 0.001$). (**#**) significantly different from the same treatment without NAC or inhibitor ($^{#}p \leq 0.05$, $^{##}p \leq 0.01$ and $^{###}p \leq 0.001$). Data from all assays are expressed as mean and standard deviation (± SD) of at least three independent experiments in duplicate.

Table 01. Cell cycle analysis by flow cytometry in promastigote forms of
***Leishmania amazonensis* treated for 24 h with T6**

Group	Sub-G0	G0/G1	S	G2/M
Untreated	3.43 ± 1.43	48.04 ± 5.68	29.02 ± 1.86	20 ± 4.43
Taxol	3.34 ± 1.24	$16.40^{***} \pm 3.83$	39.42 ± 1.78	$41.29^{***} \pm 3.65$
10 µM	11.65 ± 3.41	40.16 ± 1.86	32.03 ± 1.37	16.30 ± 2.49
20 µM	$20.84^{**} \pm 4.12$	20.97 ± 9.88	$15.47^{*} \pm 1.73$	$42.61^{***} \pm 15.57$

The data are expressed as mean percentage $\pm$ SD. (*) significantly different from untreated group ($^{*}p \leq$ 0.05, $^{**}p \leq 0.01$ and $^{***}p \leq 0.001$). Data from all assays are expressed as mean and standard deviation ($\pm$ SD) of at least three independent experiments..
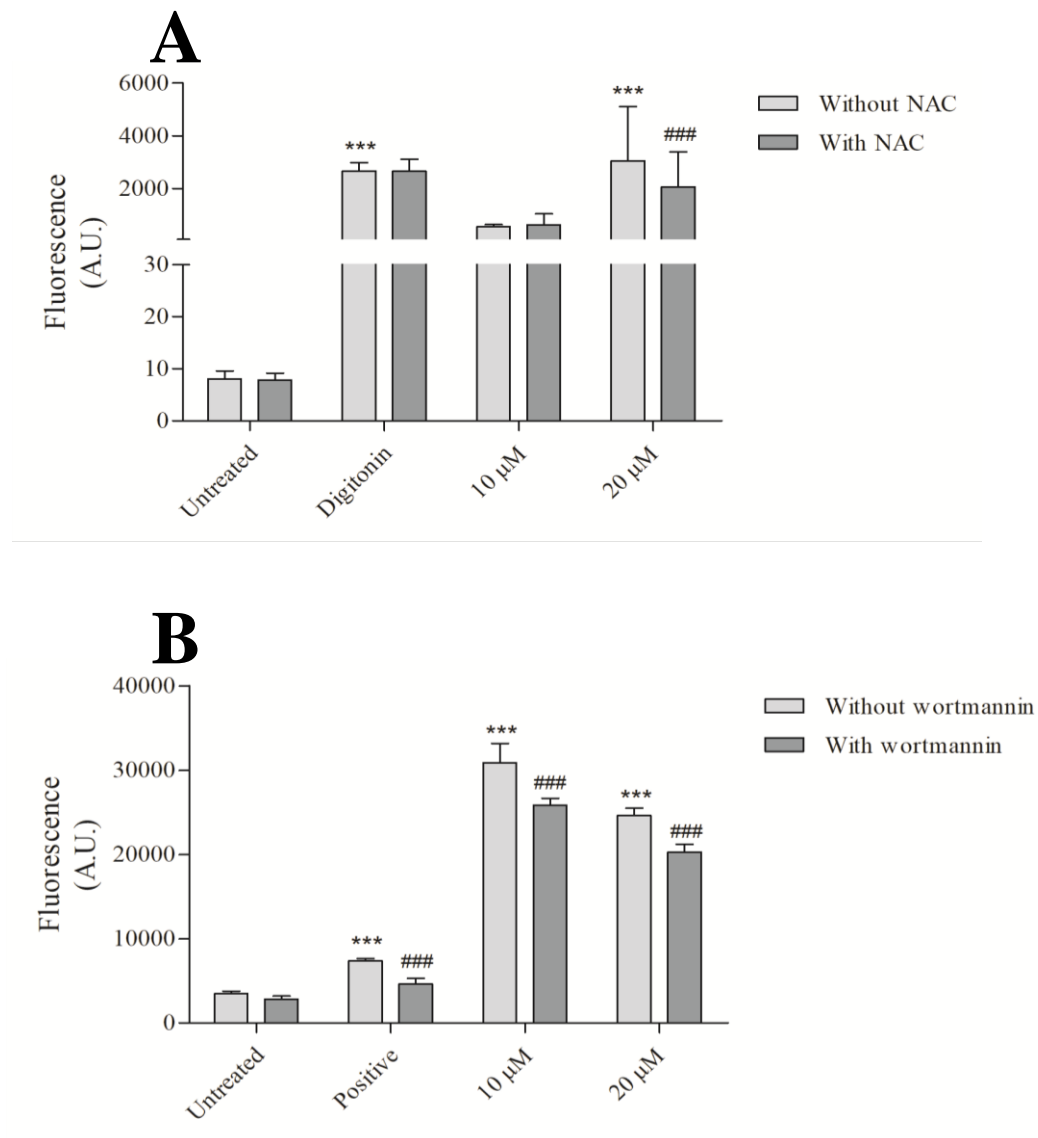
Figure 07. Elucidation of the mechanism of action in promastigote forms of _Leishmania amazonensis_ treated with T6 synthetic compound. (A) Evaluation of plasma membrane integrity and **(B)** detection of autophagic vacuoles. The pretreatment was carried out with a group of _N_-acetylcysteine antioxidant (NAC; 20 µM) or the inhibitor wortmannin (0.5 µM) autophagic vacuoles. The data are expressed as mean fluorescence ± SD. **(*)** significantly different from untreated group without NAC or wortmannin ($^{***}p \leq 0.001$). **(#)** significantly different from the same treatment without NAC or wortmannin ($^{###}p \leq 0.001$). Data from all assays are expressed as mean and standard deviation (± SD) of at least three independent experiments in triplicate.

ARTIGO CIENTÍFICO 02

Doutorando: Hélito Volpato

Orientador: Prof. Dr. Celso Vataru Nakamura

In vitro anti-*Leishmania* activity of the T6 synthetic compound encapsulated in β-(1,3)-D-glucan particles obtained from the cell wall of the yeast

Saccharomyces cerevisiae

Hélito Volpato[1], Débora Botura Scariot[2], Edna Filipa Pais Soares[3,4], Andrey Petita Jacomini[5], Fernanda Andreia Rosa[5], Maria Helena Sarragiotto[5], Tânia Ueda-Nakamura[1] Adley Forti Rubira[5], Guilherme Miranda Pereira[5], Rui Manadas[3], Alcino J. Leitão[3,4], Olga Borges[3,4], Celso Vataru Nakamura[1,2] and Maria do Céu Sousa[3,4*]

[1] Postgraduate Program in Biological Sciences, State University of Maringá (UEM), Maringá, Paraná, Brazil

[2] Postgraduate Program in Pharmaceutical Sciences, State University of Maringá (UEM), Maringá, Paraná, Brazil

[3] Faculty of Pharmacy, University of Coimbra (FFUC), Coimbra, Portugal

[4] Center for Neuroscience and Cell Biology (CNC), University of Coimbra, Coimbra, Portugal

[5] Postgraduate Program in Chemistry, State University of Maringá (UEM), Maringá, Paraná, Brazil

*Address for correspondence: Maria do Céu Sousa, Laboratory of Microbiology and Parasitology, Faculty of Pharmacy, University of Coimbra, Pole of Health Sciences, Azinhaga of Santa Comba 3000-548, Coimbra, Portugal. Phone number: +351 239 488 458. E-mail address: mcsousa@ci.uc.pt

Volpato, H. E-mail: helitovolpato2014@gmail.com

Scariot, D. B. E-mail: deborabscariot@hotmail.com

Soares, E. F. P. E-mail: edna_fps@hotmail.com

Jacomini, A. P. E-mail: andreyjacomini@hotmail.com

Rosa, F. A. E-mail: farosa@uem.br

Sarragiotto, M. H. E-mail: mhsarragiotto@uem.br

Ueda-Nakamura, T. E-mail: tunakamura@uem.br

Rubira, A. F. E-mail: afrubira@uem.br

Pereira, G. M. E-mail: gmpereira2@uem.br

Manadas, R. E-mail: rmanadas@ff.uc.pt

Leitão, A. J. E-mail: ajleitao@ff.uc.pt

Borges, O. E-mail: olga@ci.uc.pt

Nakamura, C. V. E-mail: cvnakamura@uem.br

ABSTRACT

Leishmania infantum causes visceral leishmaniasis, a form of the disease that can cause the death of the patient. Unfortunately the current drugs used in the treatment visceral leishmaniasis have several limitations, and in this way new compounds and new drug formulations are urgently needed. The objective of this study was to encapsulate a synthetic compound, the 4-[(2*E*)-*N'*-(2,2'-bithienyl-5-methylene)hydra-zinecarbonyl]-6,7-dihydro-1-phenyl-1*H*-pyrazolo[3,4-*d*]pyridazin-7-one (**T6**) in glucan-rich cell wall of *Saccharomyces cerevisae* and study the activity on *L. infantum*. We also investigated the possible mechanism of action of **T6** in the parasite. Our results showed **T6** activity in both promastigote (IC_{50} = 2.5 µg/mL) and intracellular amastigote (IC_{50} = 1.23 µg/mL) forms. We also found activity of the compound encapsulated in glucan particles against intracellular amastigote forms (IC_{50} = 8.20 µg/ml). Another interesting result was a significant decrease in J774A1 toxicity of the compound encapsulated in glucan particles (CC_{50} = >18.53 µg/mL) compared to the compound alone (IC_{50} = 2.27 µg/mL). Through electron microscopy and biochemical methodologies, we can verify that the activity of **T6** in promastigote forms of *L. infantum* is characterized by events of cell death by apoptosis like increasing of ROS production, cell shrinkage, phosphatidylserine exposure, and DNA fragmentation. We can conclude that **T6** can be considered as a promising anti-*Leishmania* compound, and that the use of glucan particles in the encapsulation of drugs is an approach to the development of new drugs.

KEYWORDS: Leishmaniasis, *Saccharomyces cerevisiae*, yeast cell wall particles; β-(1,3)-D-glucan, drug delivery; apoptosis.

1. INTRODUCTION

Leishmaniasis is a neglected tropical disease that affects several types of mammals, including humans. It is caused by parasites of the genus *Leishmania* sp, protozoa belonging to the Trypanosomatidae family (WHO, 2016). Depending on the species of the protozoan and characteristics of the immune system of the mammalian host, leishmaniasis can manifest in various clinical forms: cutaneous, diffuse, mucocutaneous or visceral (Lana et al., 2015). Visceral leishmaniasis (VL) or kala-azar is the most severe form of the disease. VL can be fatal in more than 95% of cases if there is no treatment. About 500,000 new cases are reported worldwide, with 90% occurring in Bangladesh, Brazil, Ethiopia, India, South Sudan and Sudan (Chappuis et al., 2007; Murray, Berman, Davies, & Saravia, 2005; WHO, 2016). In the new world, *L. infantum* is the etiological agent of visceral leishmaniasis (Silveira & Corbett, 2010), with an incidence of 1.9 cases per 100,000 inhabitants and a 90% mortality rate if there is no adequate treatment (Miguel, 2016). The treatment of patients with leishmaniasis is based in pentavalent antimonials, amphotericin B, paromomycin and miltefosine (Kumar et al., 2017). Unfortunately, current drugs have shown some limitations, for example, long treatment times, severe side effects, high cost, and some cases of resistance (Chappuis et al., 2007; Iwu, Jackson, & Schuster, 1994; Kumar et al., 2017). Another important fact in the severity of the disease is the accelerated development due to co-infection of patients with HIV-visceral leishmaniasis (Desjeux, 1999). Therefore, new biological active compounds and new drug formulations are urgently needed in order to have more efficacious and safe treatments. Among several possible strategies, drug vectorization has undergone considerable development over the last few years. This approach would modulate tissular and cellular distribution of the biologically active compounds and so, the side effects would be lower and the efficacy would be higher.

The drug encapsulation process promotes drug stabilization because the wall provides a physical barrier and release it in a controlled manner in biological systems (Paramera, Konteles, & Karathanos, 2011) and, in some cases, the drug-loaded particles have a higher affinity to certain cells, like macrophages, which is the case of glucan particles. The glucan particles (GPs), originating from the yeast *Saccharomyces cerevisiae* are hollow and porous particles with a size between 2-4 μm, composed mainly by β-1,3-D-glucan (Soto, Caras, Kut, Castle, & Ostroff, 2012; Soto & Ostroff, 2008). They can be obtained through a chemical procedure that extracts all the intracellular contents, leaving only one shell of yeast (Figueiredo et al., 2013; Paramera et al., 2011) that can be filled up later with the drug. The presence of β-1,3-D-glucan exposed on the surface of the particle gives to GPs an enormous advantage in the delivery of molecules,

since phagocytic cells, such as macrophages, express on their plasma membranes, the receptor dectin-1 where the glucan can bind (Brown & Gordon, 2001; Huang et al., 2012). This characteristic may be of great interest in the encapsulation of biologically active compounds for *Leishmania* sp., since its main target cell are the macrophages. This GPs can behave as microparticles, and have been used for the encapsulation of hydrophobic and hydrophilic molecules: resveratrol (Shi et al., 2008), essential oils (Bishop, Nelson, & Lamb, 1998), curcumin (Paramera et al., 2011), enzymes (Chow & Palecek, 2008), nucleic acids (Aouadi et al., 2009) and limonene (Normand, Dardelle, Bouquerand, Nicolas, & Johnston, 2005). Thus, we decided to encapsulate a synthetic compound, the 4-[(2*E*)-*N*'-(2,2'-bithienyl-5-methylene)hydra-zinecarbonyl]-6,7-dihydro-1-phenyl-1*H*-pyrazolo[3,4-*d*]pyridazin-7-one (**T6**) in GPs. Recent studies have shown promising biological activity with **T6** in *L. amazonensis*, with possible action on trypanothione reductase (TR) (Jacomini et al., 2016), an important enzyme of the antioxidant system of the parasites belonging to the *Trypanosomatidaea* family (Leroux & Krauth-Siegel, 2016). It was recognized that would be important to also test the same compound on other *Leishmania* species. Thus, our objective was to evaluate **T6** (compound alone) and **T6** loaded GPs activities in *L. infantum*, a specie responsible for visceral leishmaniasis.

2. MATERIALS AND METHODS

2.1. Chemicals

Methylthiazolyldiphenyl-tetrazolium bromide (MTT), RPMI-1640 medium, Dulbecco's Modified Eagle's Medium (DMEM), digitonin, dimethyl sulfoxide (DMSO), sodium bicarbonate (NaHCO$_3$), miltefosine, hydrogen peroxide (H$_2$O$_2$), propidium iodide (PI), 2′,7′-dichlorofluorescin diacetate (H$_2$DCFDA) and 2-propanol from Sigma-Aldrich. Agarose (Molecular Biology Grade) for gel-electrophoresis from GeneOn. Ethidium bromide solution from PluOne. Giemsa's azur eosin methylene blue solution from Merck. Penicillin-streptomycin (10,000 U/mL) from Gibco. Fetal bovine serum (FBS) from Biochrom. ApopNexin Annexin-V/FITC Apoptosis Kit from EMD Millipore. *Saccharomyces cerevisiae* (baker's yeast) from Mauripan Instant Dry Yeast. Acetone from Prolabo Chemicals. Fluo-4 AM from Molecular Probes.

2.2. Compound

The compound 4-[(2*E*)-*N'*-(2,2'-bithienyl-5-methylene)hydrazinecarbonyl]-6,7-dihydro-1-phenyl-1*H*-pyrazolo[3,4-*d*]pyridazin-7-one (**T6**; Fig 1**)** was synthesized as previously described (Jacomini et al., 2016). The bioassays were performed from a stock solution of the compound diluted in DMSO (below 1%). Physicochemical features of compound **T6**: chemical formula: $C_{21}H_{15}N_6O_2S_2$, molecular weight: 446.5, physical state: yellow solid and logP: 3.20.

2.3. Cell cultures

Promastigote forms of *Leishmania infantum* Nicolle (zymodeme MON-1) were cultured in RPMI 1640 medium (pH 7.4) supplemented with 10% FBS and maintained in incubator at 26 °C. Macrophages (RAW 264.7) were cultured in DMEM medium (pH 7.4) supplemented with 10% FBS and maintained in incubator with 5% CO_2 at 37 °C.

2.4. Preparation and characterization of glucan particles loaded with compound T6

Glucan particles preparation

Glucan particles (β-1,3-D-glucan; GPs) were prepared by suspending *Saccharomyces cerevisiae* (powder yeast) in sodium hydroxide and extracted in water bath as described by Soto (Soto & Ostroff, 2008) with some modifications. Briefly, 20 g of powder yeast cells were suspended in 200 mL of NaOH (1 M) and heating at 85 °C for 1 h. The insoluble material was collected by centrifugation (2,000 *g* for 10 min), suspended in 200 mL of NaOH (1 M) and heating at 85 °C for 1 h under rotation stirring. Then, insoluble material was collected by centrifugation, suspended in 200 mL of NaOH (1 M) and incubated only for 10 min at 85 °C under rotation stirring. After incubation, the material insoluble containing the yeast cells walls was collected by centrifugation, suspended in 200 mL of H_2O (pH 4.5; 1 mL of HCl 37% plus 1 M HCl until the correct pH) and heated at 75 °C for 1 h under rotation stirring. Then, this material was collected by centrifugation and washed three times with 200 mL of water, three times with 40 mL of isopropanol, and two times with 40 mL of acetone. In the end the acetone was discarded and dried at room temperature overnight.

Encapsulation in glucan particles

T6 was diluted in acetone, obtaining two stock solutions (100 and 500 µg/mL) for encapsulation of the compound in GPs. In Eppendorf tubes containing GPs (10 mg), 100 µL of the **T6** stock solution (100 or 500 µg/mL) was added, homogenized and incubated for 2 h at -20°C. After incubation, the tubes were opened and allowed to dry at room temperature. To obtain different concentrations of **T6** in the same mass of GPs (10 mg), several cycles (1 to 5) were performed with the two solutions of **T6** diluted in acetone. The cycles were performed in the same repeating the procedure described above.

After the encapsulation the amount of **T6** encapsulated was evaluated by an indirect way, measuring the **T6** free, not encapsulated. With that objective, acetone (1 mL) was added to the tubes with dry **T6** loaded GPs particles, immediately homogenized and centrifuged to separate the supernatant. The supernatant was transferred rapidly to a new tube and the absorbance was read at 382 nm (SHIMADZU UV-1700 PharmaSpec). The obtained absorbance was compared with the absorbance obtained in a standard **T6** curve diluted in acetone. The encapsulation efficacy (EE %) was determined using the following equation 1:

$$EE\ (\%) = \frac{total\ \textbf{T6}\ (\mu g/mL) - free\ \textbf{T6}\ in\ supernatant\ (\mu g/mL)}{total\ \textbf{T6}\ (\mu g/mL)} \times 100\ (eq.1)$$

The GPs loading capacity (LC %) with **T6** was calculated following the equation 2:

$$LC\ (\%) = \frac{total\ \textbf{T6}\ (\mu g/mL) - free\ \textbf{T6}\ in\ supernatant\ (\mu g/mL)}{total\ GPs\ (\mu g/mL)} \times 100\ (eq.2)$$

Physicochemical characterization

The zeta potential, particle size and polydispersity index of GPs and GPs+**T6** were performed in a Beckman Coulter Delsa^{TM} Nano C Particle Analyser coupled to the software Delsa^{TM} Nano Beckman Coulter. For this, the samples were diluted properly in Mili-Q water.

Fourier transforms infrared spectroscopy

Fourier transforms infrared spectroscopy (FT-IR) was performed to evaluate the possible interaction of GPs with compound **T6** in PerkinElmer Spectrum 400 FT-IR/FT-

NIR Spectrometer. For this, we performed FT-IR analysis of compound **T6** alone, blank glucan particles and glucan particles containing the synthetic compound **T6**. The samples were mixed and ground with potassium bromide and then a thin and transparent pellet was prepared before analysis.

Powder X-Ray Diffraction

Powder X-ray diffractograms (XRD) were carried out on an X-ray diffraction (XRD) instrument (Rigaku, MiniFlex600, Japan) using Cu as X-ray source with wavelength of 0.154 nm, accelerating voltage and current of 40 kV and 15 mA. The diffractograms were recorded at a rate scan of $1°$ min^{-1} and the 2θ scattered angle from 5 to 40º. For this, we perform analysis of blank glucan particles and glucan particles containing the synthetic compound **T6**.

Scanning electron microscopy and transmission electron microscopy

For morphological analysis of GPs, the dehydrated samples in increasing concentrations of acetone were metalized with gold and visualized in Shimadzu SS-550 scanning electron microscope. For ultrastructural analysis of GPs and GPs+**T6**, samples were resuspended in MilliQ water, an aliquot added on the support film grid formvar/carbon (300 mesh), dried at room temperature and visualized in transmission electron microscopy FEI-Tecnai G2 Spirit Bio Twin at 100kV.

2.5. Biological activity in *L. infantum* and macrophages cytotoxicity

Activity in promastigote

Promastigotes (1×10^6 parasites/mL) in logarithmic phase were treated with different concentrations of **T6** (100, 50, 10, 5, 1 and 0.5 µg/mL) in 96-wells plates for 72 h at 26 ºC. After treatment, 25 µL of MTT (5 mg/mL in PBS) was added and incubated for 2 h at 37 ºC. Then, parasites were centrifuged (2,000 g/5 min), supernatant removed and added DMSO. The reading was performed a microplate reader (Bio-Tek Synergy HT) at 530 nm. The 50% inhibitory concentration of parasites (IC$_{50}$) was determined in comparison to untreated control through a linear regression graph.

Activity in intracellular amastigote

The assay was performed as previously described (Kaplum et al., 2016). Briefly, peritoneal macrophages (5×10^5 cells/mL) in RPMI 1640 medium supplemented with 10% FBS were added in 24-wells plates containing round coverslips and incubated for 2 h at 37 °C. After incubation, the medium was removed, added promastigotes of *L. infantum* (3.5×10^6 parasites/mL) in stationary phase and incubated for 4 h at 34 °C. Then, non-phagocytized parasites were removed and and performed two types of treatments. For the treatment with **T6** alone, the compound diluted in RPMI 1640 medium was added in different concentrations and then incubated for 48 h at 37 °C. For treatment with GPs+**T6**, different concentrations of the compound in GPs were added and incubated for 30 min (Veras, de Chastellier, & Rabinovitch, 1992), and then the non-phagocytized particles were removed and RPMI 1640 medium was added and incubated for 48 h. After performing both types of treatments, coverslips with cells were fixed with methanol, stained with Giemsa (10% in PBS) and mounted in slides. The 50% inhibitory concentration of parasites was determined in comparison with respective control through a linear regression graph. We obtained a percentage of infection of 91.5% in the experiment.

Cytotoxicity in macrophages

RAW macrophages (5×10^5 cells/mL) were added in a 96-wells plate and incubated for 24 h at 37 °C in an atmosphere 5% CO_2 to obtain a confluent cell layer. After this period, the medium was removed, added or not different concentrations of the **T6** alone or encapsulated and incubated for 48 h. After treatment, cells were incubated with MTT (5 mg/mL in PBS) for 1 h, supernatant removed and added DMSO. The reading was performed in a microplate reader (Bio-Tek Synergy HT) at 530 nm. The 50% cytotoxic concentration (CC_{50}) was determined in comparison to untreated control through a linear regression graph.

2.6. Mechanism of action in *L. infantum* promastigotes

Morphological changes

Promastigotes (1×10^6 parasites/mL) in logarithmic phase were treated with 2.5 and 5 µg/mL of **T6** in 24-wells plates for 72 h. After the parasites were collected and centrifuged at 2,500 *g* for 10 min. The supernatant was discarded and pellet cells were fixed with glutaraldehyde (2.5%) in sodium cacodylate buffer (pH 7.2; 0.1 M) for 3 h. Then, the parasites were adhered in coverslips coated with poly-L-lysine, dehydrated in

different concentrations of ethanol, critical-point-dried with CO_2, coated with gold and observed in a FEI-Quanta 250 scanning electron microscope.

Ultrastructural changes

Promastigotes (1×10^6 parasites/mL) in logarithmic phase were treated with 2.5 and 5 μg/mL of **T6** in 24-wells plates for 72 h. After treatment, the parasites were collected and centrifuged at 2,500 *g* for 10 min. The supernatant was discarded and pellet cells were fixed with glutaraldehyde (2.5%) in sodium cacodylate buffer (pH 7.2; 0.1 M) for 3 h. Following rinsing in the same buffer, post-fixation was performed using osmium tetroxide (1%) for 1 h. After rinsing in buffer, buffer and distilled water and a final rinsing step in distilled water, aqueous uranyl acetate (1%) was added to the cells during 1 h, for contrast enhancement. After rinsing in distilled water, samples were dehydrated in a graded acetone series (70–100%). Following embedding in molten agar (2%), cell pellets were re-dehydrated in acetone (30-100%), impregnated and included in Epoxy resin (Fluka Analytical). Ultrathin sections were mounted on copper grids and stained with lead citrate (0.2%), for 7 min. Observations were carried out on FEI-Tecnai G2 Spirit Bio Twin at 100kV.

Levels H_2O_2

Promastigotes (4×10^6 parasites/mL) in logarithmic phase were treated with 2.5 and 5 μg/mL of **T6** in 24-wells plates for 24, 48 and 72 h. After treatment, the parasites were washed/resuspended in PBS buffer and incubated with H_2DCFDA (10 μM) for 45 min at room temperature protected from light. The reading was performed in microplate reader Bio-Tek Synergy HT at 488 nm of excitation and 530 nm of emission. H_2O_2 (0.25 mM) was used as positive control.

Cell volume

Promastigotes (4×10^6 parasites/mL) in logarithmic phase were treated with 2.5 and 5 μg/mL of **T6** in 24-wells plates for 24 h. The reading (1×10^4 events) was performed with BD FACSCalibur flow cytometer (FSC *vs* SSC) and data analyzed in BD CellQuest Pro software. Miltefosine (40 μM) was used as positive control.

Exposure of phosphatidylserine

Exposure of phosphatidylserine (PS) residues was determined by ApopNexin™ FITC Apoptosis Detection Kit according to the manufacturer's manual. Briefly, promastigotes (4×10^6 parasites/mL) in logarithmic phase were treated with 2.5 and 5

µg/mL of **T6** in 24-wells plates for 24 h. After treatment, the parasites were washed in PBS buffer, resuspended in binding buffer containing Annexin-V/FITC and propidium iodide (PI; 0.2 µg/mL) and incubated for 15 min at room temperature protected from light. The reading (1×10^4 events) was performed in BD FACSCalibur flow cytometer (FL1 *vs* FL3) and data analyzed with BD CellQuest Pro software. It was considered positive for annexin-V/FITC the following cell populations: annexin$^+$/PI$^-$ plus annexin$^+$/PI$^+$ (Passos, Ferreira, Soares, & Saraiva, 2015). Miltefosine (40 µM) was used as positive control.

Plasma membrane integrity

Promastigotes (4×10^6 parasites/mL) in logarithmic phase were treated with 2.5 and 5 µg/mL of **T6** in 24-wells plates for 24 h. After the parasites were washed/resuspended in PBS buffer and incubated with PI (0.2 µg/mL) for 5 min at room temperature protected from light. The reading (1×10^4 events) was performed with BD FACSCalibur flow cytometer (FL1 *vs* FL2) and data analyzed in BD CellQuest Pro software. Digitonin (40 µM) was used as positive control.

Intracellular Ca^{2+} levels

Promastigotes (4×10^6 parasites/mL) in logarithmic phase were washed/resuspended in PBS and labeled with Fluo-4 AM (5 µM) for 1 h at 26 °C in the dark. Then, the parasites were washed/resuspended in PBS and treated with 2.5 and 5 µg/mL of **T6** in a 96-well black plate. The reading was performed in microplate reader Bio-Tek Synergy HT at 494 nm of excitation and 506 nm of emission. H_2O_2 (8 mM) was used as positive control. The concentration of free Ca^{2+} was calculated using the formula:

$$Kd\frac{(F-Fmin)}{(Fmax-F)}$$

Where *Kd* is 345 nM, *F* is the fluorescence intensity of the cells, *Fmin* is the minimum fluorescence of the cells obtained by treating cells with EGTA (45 mM), and *Fmax* is maximum fluorescence of cells achieved in the presence of digitonin (40 µM) and calcium chloride (CaCl; 80 mM).

DNA fragmentation

Promastigotes (4×10^6 parasites/mL) in logarithmic phase were treated with 2.5, 5 and 10 µg/mL of **T6** in 24-wells plates for 72 h. Then parasites DNA extraction was performed through the NZY Tissue gDNA Isolation Kit, following the manufacturer's

instructions. Then, the DNA was mixed with bromophenol blue and applied to 1.5% agarose gel in Tris-acetate-EDTA buffer (TAE; 40 mM Tris-base, 20 mM acetic acid, 1 mM EDTA in deionized H_2O; pH 8.4) containing ethidium bromide (0.5 µg/mL). Electrophoretic migration occurred at 100 V for 90 min in TAE running buffer. The gel display was performed and photographed (UVITEC-UVISAVE, Alfagene) on ultraviolet light (Vilbert Lourmat). H_2O_2 (0.01, 0.05 and 0.25 mM) was used as positive control.

2.7. Statistical analysis

The data are expressed as the mean ± standard error of at least three independent experiments. The data were analyzed using One-way ANOVA analysis of variance. Significant differences among means were identified using Tukey's post hoc test. Values of p ≤ 0.05 were considered statistically significant. The statistical analyses were performed using GraphPad Prism 5 software.

3. RESULTS

3.1. Encapsulation efficiency and loading capacity

We were able to obtain GPs with different amounts of **T6**. For this, we performed several cycles of **T6** encapsulation using two stock concentrations of the compound diluted in acetone. The results of the encapsulation efficiency, encapsulated mass and loading capacity are described in Table 1.

3.2. Physico-chemical characterization

The results of the physico-chemical characterization are described in Table 2. The zeta potential, particle size and polydispersity index of GPs was of -3.94 mV, 4.86 µm and 0.31, respectively. For the particles loaded with **T6** showed zeta potential of -8.26 mV, size of 4.28 µm and polydispersity index of 0.27. By means of the zeta potential it was possible to verify an increase of the negativity in the GPs+**T6** in comparison with GPs alone.

3.3. Fourier transforms infrared spectroscopy

The FT-IR was used to verify whether **T6** was successfully incorporated in the glucan. Figure 02 shows the infrared spectrum of isolated **T6** or GPs and the corresponding GPs+**T6**. In spite of its small amount on the final particle, it is possible to verify small changes in the FT-IR spectra of the particles, when comparing with the glucan alone. These extra-peaks must be from specific groups present in the **T6** molecule, namely the aromatic ring (C=C stretch at 1600 cm^{-1} and 1475 cm^{-1}) and the amide groups (partially overlapped C=O stretch at 1706 cm^{-1} and N-H bending at 1659 cm^{-1}).

3.4. Powder X-Ray Diffraction

The encapsulation of **T6** into GPs was also investigated by XRD analysis. The XRD diffractogram of the GPs (Fig. 03 - A) shows a very broad peak in ca. 20 ° which is attributed to the polymeric structures of the polysaccharide and indicates the low crystallinity of the particles (Veverka et al., 2014). The diffractogram of the synthetic compound **T6** shows very intense and thin XRD peaks indicating a very crystalline structure (Fig 03 - B). Figure 03 - C shows that the diffractogram of the GPs+**T6** sample retains mainly the XRD pattern from pure GPs with very small peaks at ca. 8.7°, 15.1°, 23.3° and 27.9° which can be due to the **T6** compound. These results are more evident when the diffractogram of GPs is subtracted from the GPs+**T6** (Fig. 03 - D) and suggest that **T6** was successfully incorporated in GPs particles.

3.5. Scanning and transmission electron microscopy

Through analysis by SEM and TEM (Fig. 04), we observed normal characteristics of the glucan particles extracted from the yeast cell wall *S. cerevisiae*. In order to analyze a possible structural difference after the encapsulation, we decided to observe the empty particles (GPs) and the particles loaded with the synthetic compound **T6** (GPs+**T6**). By TEM it was not possible to verify structural difference between both samples. By TEM it was not possible to verify structural difference between the two samples. This can be explained due to the size of the particles, because it has micrometric size. For an analysis of the incorporation of the compound in the particles, it would be more viable an analysis in the TEM in nanometric level.

3.6. Biological activity in *L. infantum* and macrophages cytotoxicity

*Biological activity in L. infantum and cytotoxicity in RAW of compound **T6***

In this work, we performed the activity of the compound in promastigotes and intracellular amastigotes of *L. infantum* (the specie responsible for visceral leishmaniasis) and obtained IC_{50} of 2.5 and 1.23 µg/mL, respectively (Table 05; Fig. 05). Unfortunately, compound **T6** demonstrated toxicity in mammalian cells (macrophages RAW), with a CC_{50} of 2.8 µg/mL (Table 03).

***T6** encapsulated demonstrates anti-amastigote activity in L. infantum without cytotoxicity in RAW macrophages*

We obtained in amastigotes of *L. infantum* the IC_{50} of 8.2 µg/mL of the encapsulated compound, a value corresponding to 6 times higher than in the free compound (1.23 µg/mL) (Table 03; Fig 05). In turn, no toxicity in macrophages RAW of encapsulated **T6** was observed, even at the highest concentration tested (CC_{50}: >152 µg/mL). GPs-free were tested in macrophages and showed no toxicity (CC_{50}: > 20,000 µg/mL; Table 03).

3.7. Mechanism of action of T6 in *L. infantum* promastigotes

***T6** induces morphological changes*

Scanning electron microscopy was performed in the search for possible morphological alteration in promastigotes of *L. infantum* treated with **T6** (Fig. 06). Untreated parasites showed normal characteristics, such as elongated body, integral membrane, single and long flagellum (Fig.06 - A). Parasites treated with 2.5 µg/mL showed reduction and rounding of the cell body (Fig. 06 - B and C). Additionally, the treatment with 5 µg/mL showed an evident alteration in the plasma membrane (Fig. 06 - D, E and F).

***T6** induces ultrastructural changes*

Transmission electron microscopy was performed in order to verify ultrastructural alteration in promastigote forms of *L. infantum* treated with **T6** (Fig. 07). Untreated control demonstrated normal characteristics of the protozoan, such as elongated body, the

presence of a nucleus, normal mitochondria and kinetoplast, and the presence of flagellar pocket with free flagella (Fig. 07 – A). Treatment with 2.5 µg/mL of **T6** showed damage to the parasite, such as alteration in the nuclear envelope, disorganization in the Golgi complex, and the presence of concentric membrane structures and autophagic vacuoles (Fig. 07 – B, C and D). At the concentration of 5 µg/mL, it was possible to observe change in nucleus, decrease in mitochondrial density and disorganization of the endoplasmic reticulum (Fig. 07 - E and F).

T6 induces increased levels of H_2O_2

In promastigotes **T6** at the concentration of 5 µg/mL caused an increase of ROS in 278% after 72 h of treatment, compared to the untreated control (Fig. 08 - A). H_2O_2 (0.25 mM) was used as a positive control and caused a significant increase at all times tested.

T6 reduces cell volume

Results obtained by analysis in flow cytometer showed that promastigotes of *L. infantum* treated with 2.5 µg/mL of **T6** for 24 h induced a slight decrease in cell volume (Fig. 08 - B). This change was observed in the microscope during the experiments (data not shown). The apoptosis inducer miltefosine (40 µM) showed similar result.

T6 induces exposure of phosphatidylserine

Our results by flow cytometry demonstrate that **T6** in both tested concentrations per 24 h induces an increase of exposure of PS in relation to the untreated control (8 and 19.4 times) (Fig. 08 - C). Miltefosine (40 µM) considered an inducer of cell death by apoptosis was used as positive control, and demonstrated the same effect.

T6 does not induce changes in the plasma membrane

The results show that the **T6** did not significantly alter the permeability of the plasma membrane of the parasite treated for 24 h (Fig. 08 - D). Positive control was performed with digitonin (40 µM), a powerful detergent capable of solubilizing the lipids present in the membranes, facilitating propidium iodide binding in the DNA of the parasite**.**

T6 induces increase in intracellular Ca^{2+} level

Our results demonstrated a significant increase of intracellular calcium in both of the two concentrations tested of **T6**. H_2O_2 (8mM) was used as an inducer of oxidative stress, and thus demonstrated increase in calcium levels compared to the untreated group.

After 1 h of treatment with 2.5 and 5 µg/mL of **T6**, there was an increase of intracellular calcium of 478% and 843% respectively (Fig. 08 – E).

T6 induces DNA fragmentation

The result showed DNA fragmentation in parasite treated with **T6** (5 and 10 µg/mL) for 72 h (Fig. 9). H_2O_2 (0.25 mM) was used as DNA fragmentation-inducing, and the results were positive.

4. DISCUSSION

In the search for new anti-*Leishmania* drugs, synthetic compounds have been targets of biological studies (Mendes et al., 2016; Volpato et al., 2013). Recently, activity of a synthetic compound in *Leishmania amazonensis*, 4-[(2*E*)-*N'*-(2,2'-bithienyl-5-methylene)hydrazinecarbonyl]-6,7-dihydro-1-phenyl-1*H*-pyrazolo[3,4-*d*]pyridazin-7-one (**T6)** was demonstrated (Jacomini et al., 2016). In this way, the present work aimed to evaluate **T6** activity in *L. infantum*, a species responsible for the most severe form of the disease, visceral leishmaniasis.

Through the results obtained, **T6** showed a promising activity in both promastigote and intracellular amastigote forms of *L. infantum*. Unfortunately, **T6** was tested in RAW macrophages and presented a considered toxicity. In view of the presented problem, we decided to perform the encapsulation of compound that was biologically active on *L. infantum*, with the aim of reducing the toxicity presented in mammalian cells. We decided to perform encapsulation on GPs chemically extracted from the cell wall of yeast *S. cerevisiae*. GPs have immunomodulatory action, being capable of activating macrophages, neutrophils and dendritic cells, thus promoting the increased production of pro-inflammatory cytokines (IL-6 and IL-8), tumor necrosis factor and nitric oxide (Czop, 1986; Ross, Vetvicka, Yan, Xia, & Vetvicková, 1999; Williams, Mueller, & Browder, 1996). All these immunological responses are due to the presence of two major receptors, dectin-1 and complement receptor 3, both present in the plasma membrane of phagocytic cells, for example the macrophages (Brown & Gordon, 2001; Huang et al., 2012), cells present in regions affected by *L. infantum* infection such as liver and spleen.

Through the results obtained, it was possible to incorporate the compound into GPs, but the percentage of encapsulation and mass were not satisfactory, as demonstrated by other encapsulation processes. This can be explained by performing the washing

process after encapsulation, since both steps (encapsulation and washing) were performed with the same solvent, acetone. After performing biological activity *in vitro*, the compound loaded in GPs maintained activity in intracellular amastigote forms of *L. infantum*. Interestingly, particles loaded with the highest concentration of **T6** did not cause toxicity in RAW macrophages, as evaluated in tests done with the compound alone. The activity in intracellular forms of the parasite and low toxicity of the encapsulated compound can be explained due to the fact that the particles are easily phagocytosed due to the presence of the membrane receptors directed to the phagolysosomes (Veras et al., 1992), being the site of the degradation of the particles by the lysosomal enzymes, and thus releasing the active compound. Another reason for the biological activity maintained in the parasite is the immunomodulatory response of GPs after phagocytosis (Czop, 1986; Ross et al., 1999; Williams et al., 1996). The low solubility of the compound, seen in the *in vitro* tests, may also explain the minimized toxic effects in mammalian cells.

The efficiency of the encapsulation system in GPs to decrease **T6** cytotoxicity, even with low encapsulation efficiency, stimulates a more in-depth study, since the biological activity remained satisfactory on intracellular amastigote forms. Moreover, the fact that encapsulation of a poorly soluble compound also makes this system a promising form for the delivery and targeting of bioactive molecules.

Due to the promising biological activity presented by **T6** in both evolutionary forms of *L. infantum*, we decided to evaluate the possible mechanism of action that culminates in the cellular death of the parasite. Therefore, we perform methodologies that involve morphological, ultrastructural and biochemical parameters. Apoptosis is a type of programmed cell death that leads to morphological and biochemical changes in cells, for example, decrease in cell volume, DNA fragmentation, formation of apoptotic bodies, reduction of mitochondrial membrane potential, opening of mitochondrial membrane permeability pores, externalization of phosphatidylserine, release of pro-apoptotic proteins (cytochrome c) and activation of proteases (caspases) (Galluzzi et al., 2012; Orrenius, Gogvadze, & Zhivotovsky, 2007; Ott, Gogvadze, Orrenius, & Zhivotovsky, 2007). Our results demonstrated characteristics of cell death through apoptosis, as it was observed by flow cytometry and scanning electron microscopy a decrease in the cellular volume of the parasites treated with **T6**. By flow cytometry, it was also possible to verify an increase in the externalization of phosphatidylserine residues after **T6** treatment for 24 h. Another evidence of apoptosis cell death caused by the treatment with the synthetic compound was DNA fragmentation, seen through agarose gel electrophoresis. In addition to apoptotic death, we also evaluated death by necrosis, a type of cell death characterized

mainly by increased cytoplasmic volume and rupture of the plasma membrane, leading to an inflammatory response (Zielonka et al., 2009). Propidium iodide is an excellent indicator of plasma membrane integrity, due to its ability to bind to the nucleic acids of cells with the ruptured membrane. Our results did not show a significant alteration of the plasma membrane of the parasite treated for 24 h. It was also possible demonstrate for transmission electron microscopy that the treatment for 72 h did not cause disruption of the plasma membrane of the parasite. Both results demonstrate the absence of necrotic cell death in promastigote forms of *L. infantum* treated with compound **T6**. By means of fluorimeter techniques, it was possible to verify other changes in the parasites after treatment with **T6**. We have seen an increase in H_2O_2 and intracellular Ca^{2+}. ROS are molecules that can react with proteins, lipids and nucleic acids, and thus causing severe cellular damage leading to activation of apoptosis (Redza-Dutordoir & Averill-Bates, 2016). Intracellular Ca^{2+} plays a key role during the initiation and activation of apoptotic cell death (Redza-Dutordoir & Averill-Bates, 2016).

In comparison to the mechanism of action of the current treatments, we verified that **T6** demonstrated differences and similarities in cellular targets. It has been reported that amphotericin B alters the parasite membrane steroids, and in this way causes a loss of permeability barrier over small metabolites (Saha et al. 1986). About miltefosine, studies demonstrate that this drug inhibits the synthesis of phosphatidylcholine, alters mitochondria through the inhibition of cytochrome c oxidase and induces cell death by apoptosis via DNA fragmentation (Pinto-Martinez, 2018). Regarding paramomicin, an antibiotic, studies report that this drug acts on the inhibition of parasite multiplication by acting on RNA synthesis, modification of polar lipids and membrane fluidity (Maarouf et al, 1997) alteration of mitochondrial membrane potential and synthesis of cytoplasmic and mitochondrial proteins (Jhingran et al, 2009). Through these current results we can propose that **T6** could be used together with some of the current treatment of patients with leishmaniasis with the purpose of causing a synergistic effect, and thus increase the activity on the parasite.

5. CONCLUSION

We conclude that **T6** synthetic compound demonstrated a promising *in vitro* activity in promastigotes and intracellular amastigotes of *Leishmania infantum*, being this activity due to changes that cause cell death by apoptosis. Another important factor in this work was the successful use of the encapsulation technique of the compound in glucan

particles extracted from the yeast cell wall in order to decrease the cytotoxicity presented with the free **T6** compound. Further studies should be performed, including *in vivo* analysis of **T6**-loaded particles and deepening of the mechanism of action in the parasite with the aim of developing a more efficient drug for the treatment of patients with visceral leishmaniasis.

6. REFERENCES

Aouadi, M., Tesz, G. J., Nicoloro, S. M., Wang, M., Chouinard, M., Soto, E., Czech, M. P. (2009). Orally delivered siRNA targeting macrophage Map4k4 suppresses systemic inflammation. *Nature*, *458*(7242), 1180–1184. doi.org/10.1038/nature07774

Bishop, J. R. P., Nelson, G., & Lamb, J. (1998). Microencapsulation in yeast cells. *Journal of Microencapsulation*, *15*(6), 761–773. doi.org/10.3109/02652049809008259

Brown, G. D., & Gordon, S. (2001). Immune recognition: A new receptor for β-glucans. *Nature*, *413*(6851), 36–37. doi.org/10.1038/35092620

Chappuis, F., Sundar, S., Hailu, A., Ghalib, H., Rijal, S., Peeling, R. W., Boelaert, M. (2007). Visceral leishmaniasis: what are the needs for diagnosis, treatment and control? *Nature Reviews Microbiology*, *5*(11), S7–S16. doi.org/10.1038/nrmicro1748

Chow, C.-K., & Palecek, S. P. (2008). Enzyme Encapsulation in Permeabilized *Saccharomyces cerevisiae* Cells. *Biotechnology Progress*, *20*(2), 449–456. doi.org/10.1021/bp034216r

Czop, J. K. (1986). The role of β-glucan receptors on blood and tissue leukocytes in phagocytosis and metabolic activation. *Pathology and Immunopathology Research*, *5*(3–5), 286–96. Retrieved from http://www.ncbi.nlm.nih.gov/pubmed/3037509

Desjeux, P. (1999). Global control and *Leishmania* HIV co-infection. *Clinics in Dermatology*, *17*(3), 317–325. doi.org/10.1016/S0738-081X(99)00050-4

Figueiredo, S., Cutrin, J. C., Rizzitelli, S., De Luca, E., Moreira, J. N., Geraldes, C. F. G. C., Terreno, E. (2013). MRI tracking of macrophages labeled with glucan particles entrapping a water insoluble paramagnetic Gd-based agent. *Molecular Imaging and Biology*, *15*(3), 307–315. doi.org/10.1007/s11307-012-0603-x

Galluzzi, L., Vitale, I., Abrams, J. M., Alnemri, E. S., Baehrecke, E. H., Blagosklonny, M. V, Kroemer, G. (2012). Molecular definitions of cell death subroutines: recommendations of the Nomenclature Committee on Cell Death 2012. *Cell Death and Differentiation*, *19*(1), 107–120. doi.org/10.1038/cdd.2011.96

Huang, H., Ostroff, G. R., Lee, C. K., Agarwal, S., Ram, S., Rice, P. A., Levitz, S. M.

(2012). Relative contributions of dectin-1 and complement to immune responses to particulate β-glucans. *The Journal of Immunology*, *189*(1), 312–317. doi.org/10.4049/jimmunol.1200603

Iwu, M. M., Jackson, J. E., & Schuster, B. G. (1994). Medicinal plants in the fight against leishmaniasis. *Parasitology Today (Personal Ed.)*, *10*(2), 65–8. Retrieved from http://www.ncbi.nlm.nih.gov/pubmed/15275504

Jacomini, A. P., Silva, M. J. V., Silva, R. G. M., Gonçalves, D. S., Volpato, H., Basso, E. A., Rosa, F. A. (2016). Synthesis and evaluation against *Leishmania amazonensis* of novel pyrazolo[3,4-d]pyridazinone-N-acylhydrazone-(bi)thiophene hybrids. *European Journal of Medicinal Chemistry*, *124*. doi.org/10.1016/j.ejmech.2016.08.048

Jhingran, A., Chawla, B., Saxena, S., Barrett, M. P., Madhubalaa, R. (2009). aromomycin: uptake and resistance in *Leishmania donovani*. *Molecular and Biochemical Parasitology*, *164*(2), 111-117. doi.org/10.1016/j.molbiopara.2008.12.007

Kaplum, V., Cogo, J., Sangi, D. P., Ueda-Nakamura, T., Corrêa, A. G., & Nakamura, C. V. (2016). *In vitro* and *in vivo* activities of 2,3-diarylsubstituted quinoxaline derivatives against *Leishmania amazonensis*. *Antimicrobial Agents and Chemotherapy* , *60*(6), 3433–3444. doi.org/10.1128/AAC.02582-15

Kumar, V., Yadav, S., Soumya, N., Kumar, R., Babu, N. K., & Singh, S. (2017). Biochemical and inhibition studies of glutamine synthetase from *Leishmania donovani*. *Microbial Pathogenesis*, *107*, 164–174. doi.org/10.1016/j.micpath.2017.03.024

Lana, R. S., Michalsky, É. M., Fortes-Dias, C. L., França-Silva, J. C., Lara-Silva, F. de O., Rocha Lima, A. C. V. M. da, … Dias, E. S. (2015). Phlebotomine sand fly fauna and *Leishmania* infection in the Vicinity of the Serra do Cipó National Park, a Natural Brazilian Heritage Site. *BioMed Research International*, *2015*, 1–9. doi.org/10.1155/2015/385493

Leroux, A. E., & Krauth-Siegel, R. L. (2016). Thiol redox biology of trypanosomatids and potential targets for chemotherapy. *Molecular and Biochemical Parasitology*, *206*(1), 67–74. doi.org/10.1016/j.molbiopara.2015.11.003

Maarouf, M., Spencer, F. L., Robert-Gero, M. B. (1997). Biochemical alterations in

paromomycin-treated *Leishmania donovani* promastigotes. *Parasitology Research*, *83*(2), 198–202. doi.org/10.1007/s004360050232

Mendes, E. A., Desoti, V. C., Silva, S. de O., Ueda-Nakamura, T., Dias Filho, B. P., Yamada-Ogatta, S. F., Nakamura, C. V. (2016). C5 induces different cell death pathways in promastigotes of *Leishmania amazonensis*. *Chemico-Biological Interactions*, *256*, 16–24. doi.org/10.1016/j.cbi.2016.06.018

Miguel, P. S. B. (2016). Visceral leishmaniasis: a brazilian perspective. (R. R. Vitorino, Ed.), *Journal of Tropical Diseases & Public Health*. OMICS International.,. doi.org/10.4172/2329-891X.1000202

Murray, H. W., Berman, J. D., Davies, C. R., & Saravia, N. G. (2005). Advances in leishmaniasis. *The Lancet*, *366*(9496), 1561–1577. doi.org/10.1016/S0140-6736(05)67629-5

Normand, V., Dardelle, G., Bouquerand, P.-E., Nicolas, L., & Johnston, D. J. (2005). Flavor encapsulation in yeasts: limonene used as a model system for characterization of the release mechanism. *Journal of Agricultural and Food Chemistry*, *53*(19), 7532–7543. doi.org/10.1021/jf0507893

Orrenius, S., Gogvadze, V., & Zhivotovsky, B. (2007). Mitochondrial oxidative stress: implications for cell death. *Annual Review of Pharmacology and Toxicology*, *47*, 143–83. doi.org/10.1146/annurev.pharmtox.47.120505.105122

Ott, M., Gogvadze, V., Orrenius, S., & Zhivotovsky, B. (2007). Mitochondria, oxidative stress and cell death. *Apoptosis*, *12*(5), 913–922. doi.org/10.1007/s10495-007-0756-2

Paramera, E. I., Konteles, S. J., & Karathanos, V. T. (2011). Microencapsulation of curcumin in cells of *Saccharomyces cerevisiae*. *Food Chemistry*, *125*(3), 892–902. doi.org/10.1016/j.foodchem.2010.09.063

Passos, C. L. A., Ferreira, C., Soares, D. C., & Saraiva, E. M. (2015). Leishmanicidal effect of synthetic trans-resveratrol analogs. *PLOS ONE*, *10*(10), e0141778. doi.org/10.1371%2Fjournal.pone.0141778

Pinto-Martinez, A. K., Rodriguez-Durán, J., Serrano-Martin, X,, Hernandez-Rodriguez, V., Benaim, G. (2018). Mechanism of action of miltefosine on *Leishmania donovani* involves the impairment of acidocalcisome function and the activation of the

sphingosine-dependent plasma membrane Ca^{2+} channel. *Antimicrob Agents Chemother*, *62*(1), n. pag. doi.org/10.1128/AAC.01614-17

Redza-Dutordoir, M., & Averill-Bates, D. A. (2016). Activation of apoptosis signalling pathways by reactive oxygen species. *Biochimica et Biophysica Acta (BBA) - Molecular Cell Research*, *1863*(12), 2977–2992. doi.org/10.1016/j.bbamcr.2016.09.012

Ross, G. D., Vetvicka, V., Yan, J., Xia, Y., & Vetvicková, J. (1999). Therapeutic intervention with complement and β-glucan in cancer. *Immunopharmacology*, *42*(1–3), 61–74. Retrieved from http://www.ncbi.nlm.nih.gov/pubmed/10408367

Saha, A. K., Mukherjee, T., Bhaduri, A (1986). Mechanism of action of amphotericin B on *Leishmania donovani* promastigotes. *Molecular and Biochemical Parasitology*, *19*(3), 195-200. doi.org/10.1016/0166-6851(86)90001-0

Shi, G., Rao, L., Yu, H., Xiang, H., Yang, H., & Ji, R. (2008). Stabilization and encapsulation of photosensitive resveratrol within yeast cell. *International Journal of Pharmaceutics*, *349*(1–2), 83–93. doi.org/10.1016/j.ijpharm.2007.07.044

Silveira, F. T., & Corbett, C. E. P. (2010). *Leishmania chagasi* Cunha & Chagas, 1937: indigenous or introduced? A brief review. *Revista Pan-Amazônica de Saúde*, *1*(2), 143–147. doi.org/10.5123/S2176-62232010000200018

Soto, E. R., Caras, A. C., Kut, L. C., Castle, M. K., & Ostroff, G. R. (2012). Glucan particles for macrophage targeted delivery of nanoparticles. *Journal of Drug Delivery*, *2012*, 143524. doi.org/10.1155/2012/143524

Soto, E. R., & Ostroff, G. R. (2008). Characterization of multilayered nanoparticles encapsulated in yeast cell wall particles for DNA delivery. *Bioconjugate Chemistry*, *19*(4), 840–848. doi.org/10.1021/bc700329p

Veras, P. S., de Chastellier, C., & Rabinovitch, M. (1992). Transfer of zymosan (yeast cell walls) to the parasitophorous vacuoles of macrophages infected with *Leishmania amazonensis*. *The Journal of Experimental Medicine*, *176*(3), 639–46. Retrieved from http://www.ncbi.nlm.nih.gov/pubmed/1512533

Veverka, M., Dubaj, T., Gallovič, J., Jorík, V., Veverková, E., Mičušík, M., & Šimon, P. (2014). β-glucan complexes with selected nutraceuticals: synthesis, characterization, and stability. *Journal of Functional Foods*, *8*, 309–318.

doi.org/10.1016/J.JFF.2014.03.032

Volpato, H., Desoti, V. C., Cogo, J., Panice, M. R., Sarragiotto, M. H., Silva, S. de O., Nakamura, C. V. (2013). The effects of N-butyl-1-(4-dimethylamino)phenyl-1,2,3,4-tetrahydro-β-carboline-3-carboxamide against *Leishmania amazonensis* are mediated by mitochondrial dysfunction. *Evidence-Based Complementary and Alternative Medicine : eCAM*, *2013*, 874367. doi.org/10.1155/2013/874367

WHO. (2016). Leishmaniasis, 1–5.

Williams, D. L., Mueller, A., & Browder, W. (1996). Glucan-based macrophage stimulators. *Clinical Immunotherapeutics*, *5*(5), 392–399. doi.org/10.1007/BF03259335

Zielonka, J., Kalyanaraman, B., Zhang, X., Zhang, K., Zamaraeva, M. V, Sabirov, R. Z., Melino, G. (2009). Classification of cell death: recommendations of the Nomenclature Committee on Cell Death 2009. *Cell Death and Differentiation*, *16*(1), 3–11. https://doi.org/10.1038/cdd.2008.150
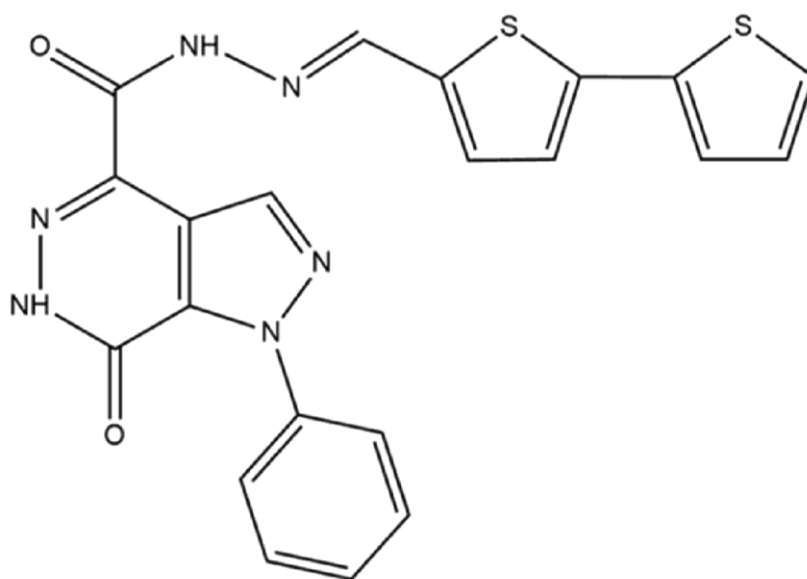
7. FIGURES E TABLES

Figure 1. Chemical structure of compound of the compound 4-[(2*E*)-*N'*-(2,2'-bithienyl-5-methylene)hydrazinecarbonyl]-6,7-dihydro-1-phenyl-1*H*-pyrazolo[3,4*d*]pyridazin-7-one **(T6)**. Chemical formula: $C_{21}H_{15}N_6O_2S_2$. Molecular weight: 446.5.

Table 01. Encapsulation efficiency (%)

Cycle(s)	[100 μg/mL]	[500 μg/mL]
1	36.08 ± 3.90	34.29 ± 12.83
2	46.14 ± 1.96	50.97 ± 20.50
3	54.58 ± 10.42	57.13 ± 21.69
4	56.01 ± 7.49	60.25 ± 18.90
5	59.17 ± 4.90	60.95 ± 18.41

Table 02. Encapsulated mass (μg of T6/mg of GPs)

Cycle(s)	[100 μg/mL]	[500 μg/mL]
1	0.36 ± 0.04	1.71 ± 0.64
2	0.92 ± 0.04	5.09 ± 2.05
3	1.63 ± 0.31	8.56 ± 3.24
4	2.23 ± 0.29	12.05 ± 3.78
5	2.95 ± 0.24	15.24 ± 4.61

Table 03. Encapsulated T6 content (%)

Cycle(s)	[100 μg/mL]	[500 μg/mL]
1	0.0036 ± 0.0004	0.0171 ± 0.0064
2	0.0092 ± 0.0004	0.0509 ± 0.0205
3	0.0163 ± 0.0031	0.0856 ± 0.0324
4	0.0223 ± 0.0029	0.1205 ± 0.0378
5	0.0295 ± 0.0024	0.1525 ± 0.0461

Table 04. Physico-chemical characterization: Zeta potential, particle size and polydispersity index

Sample	Zeta Potential (mV)	Particle size (μm)	Polydispersity Index
GPs	-3.94 ± 1.80	4.86 ± 0.0158	0.31 ± 0.05
GPs+T6	- 8.26 ± 2.75	4.28 ± 0.163	0.27 ± 0.08

Table 05. Biological activity of T6 compound on *Leihmania infantum* and cytotoxicity on macrophage RAW cells (µg/mL)

Compound	$^{pro}IC_{50}$	$^{ama}IC_{50}$	CC_{50}	^{pro}SI	^{ama}SI
T6	2.5 ± 0.5	1.2 ± 0.3	2.8 ± 0.2	1.1	2.2
GPs	nd	nd	>20000	nd	nd
GPs+T6	nd	8.2 ± 1.4	>152.3	nd	>18.5

$^{pro}IC_{50}$: inhibitory concentration 50% of the promastigote forms treated for 72 h; $^{ama}IC_{50}$: inhibitory concentration 50% of the intracellular amastigote forms treated for 48 h; CC_{50}: cytotoxic concentration for 50% of macrophage; ^{pro}SI: selectivity index in promastigote forms ($CC_{50}/^{pro}IC_{50}$); ^{ama}SI: selectivity index in amastigote forms ($CC_{50}/^{ama}IC_{50}$); nd: no determined.
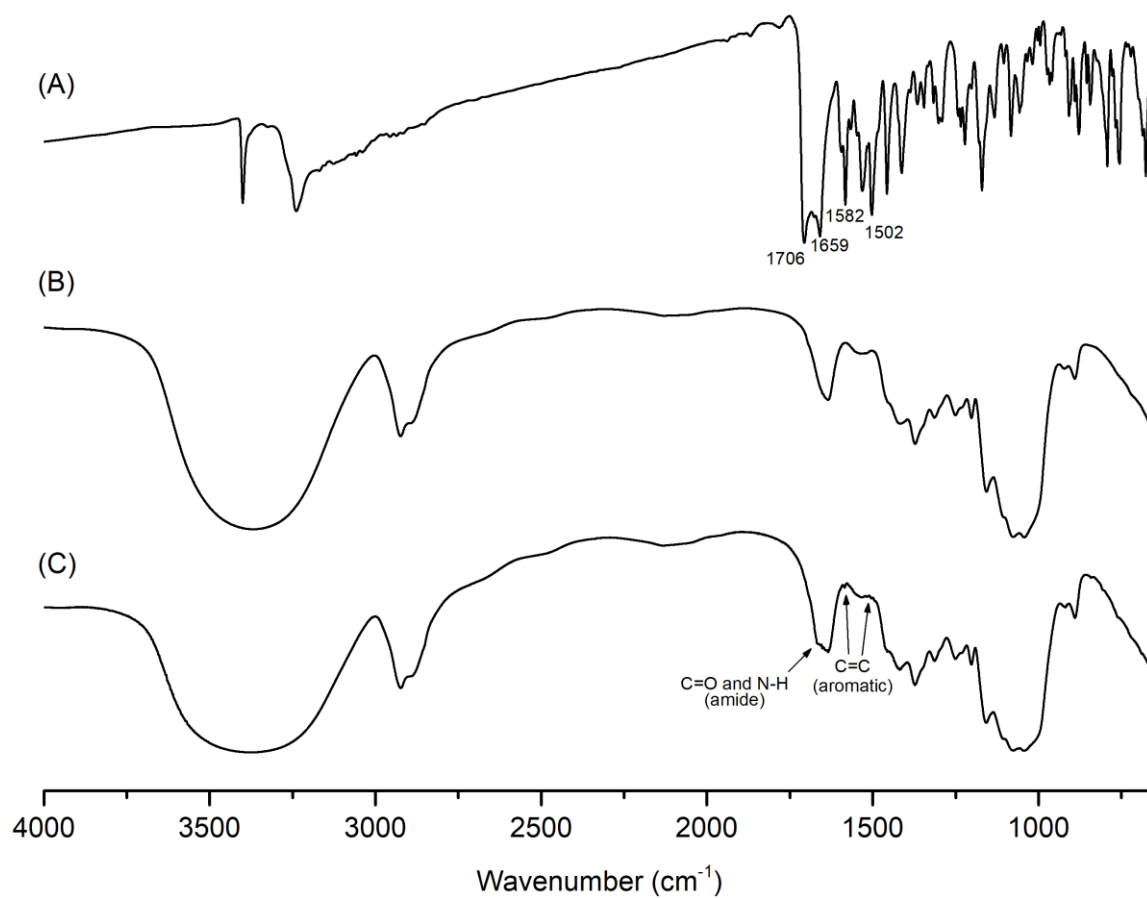
Figure 02. Fourier transform infrared spectroscopy of compound **T6**, glucan particles (**GPs**) and **T6** encapsulated in glucan particles (**GPs+T6**).
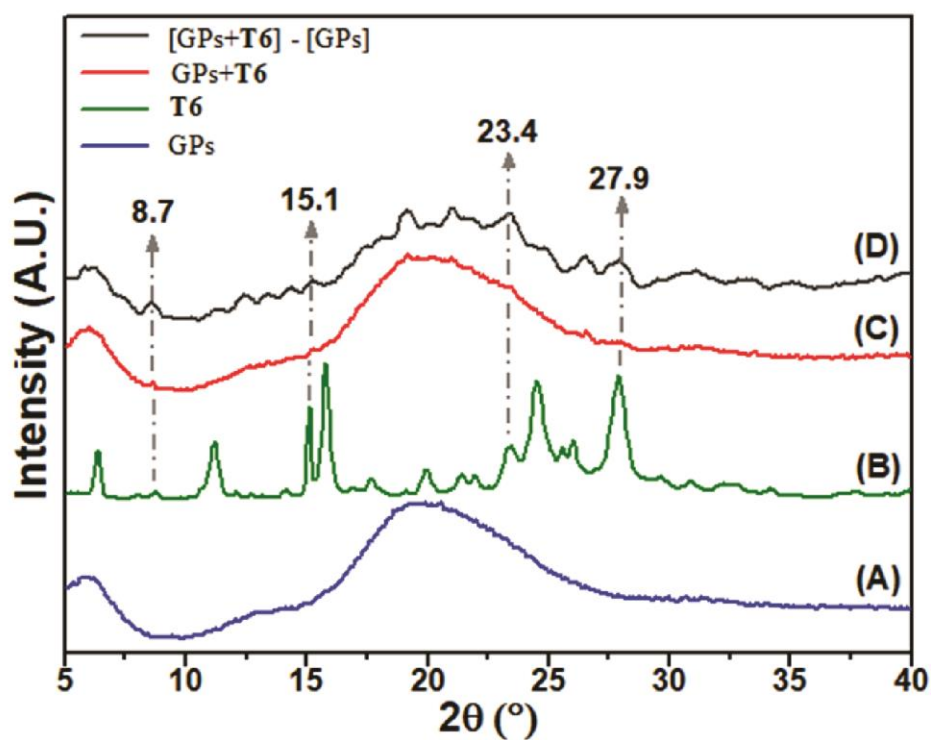
Figure 3. X-ray diffraction (XRD) patterns of **(A)** GPs, **(B)** T6, **(C)** GPs+T6 and **(D)** curve obtained when GPs diffractogram is subtracted from GPs+T6 diffractogram.
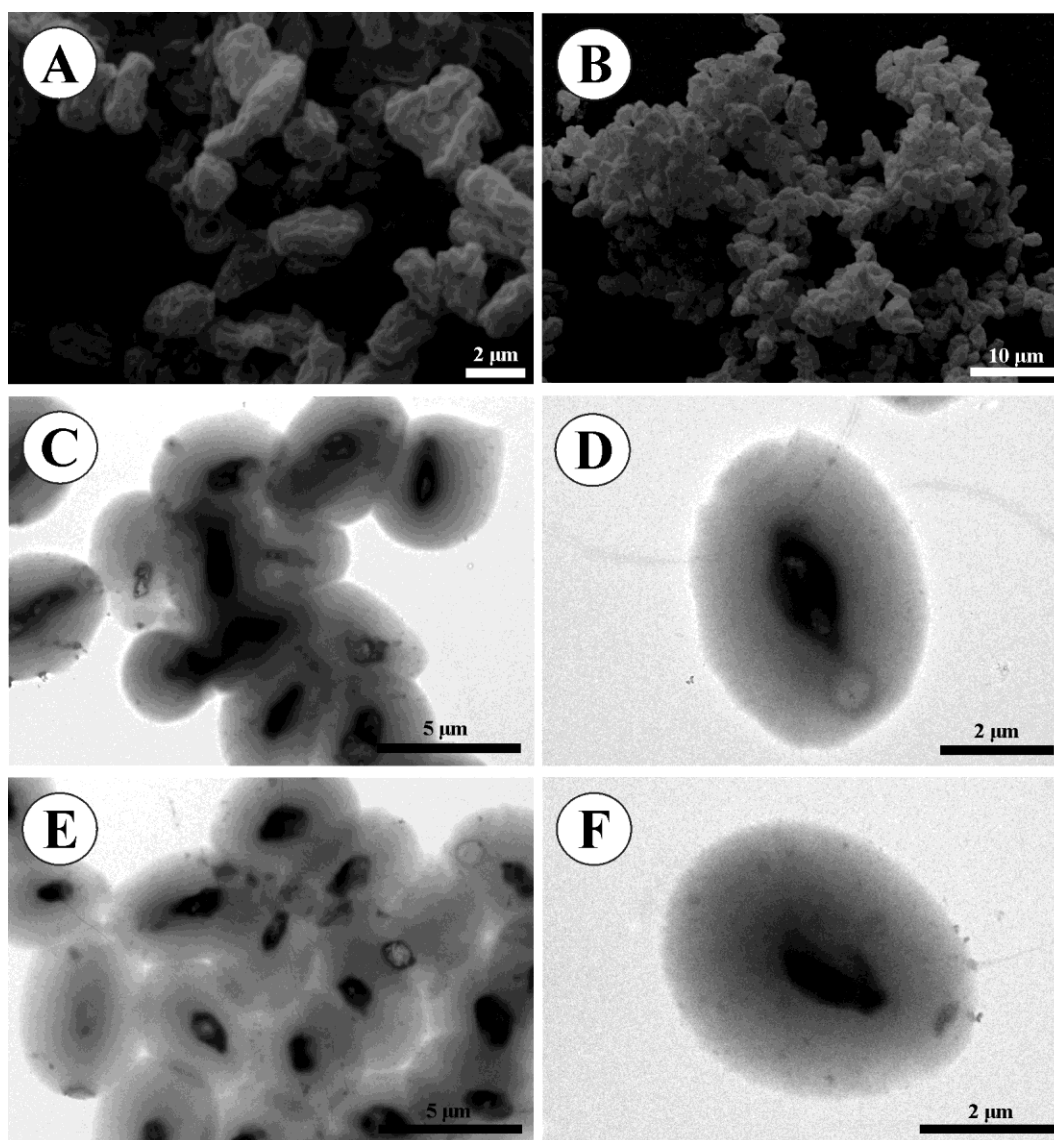
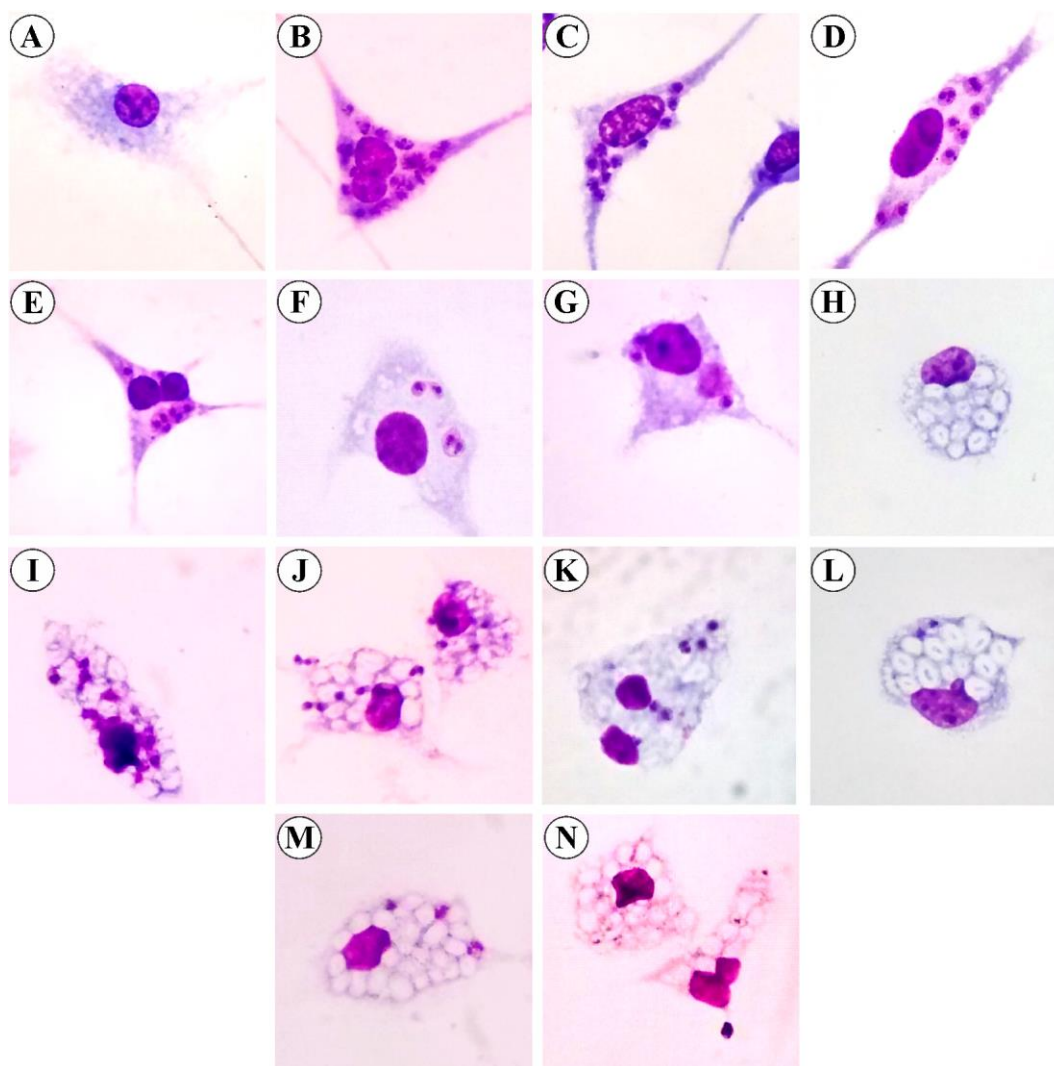**Figure 04.** Scanning electron microscopy of **GPs** (**A** and **B**) and transmission electron microscopy of **GPs (C-D)** and **GPs+T6 (E** and **F)**.

Figure 05. Biological activity in intracellular amastigotes of *L. infantum*. Cells were treated with different concentrations of **T6**, **GPs** or **GPs**+**T6** for 48 h. **(A)** non-infected and untreated, **(B)** infected and untreated. **(C-G)** infected and treated with **T6**: **(C)** 0.1 µg/mL, **(D)** 0.5 µg/mL, **(E)** 1 µg/mL, **(F)** 2.5 µg/mL and **(G)** 5 µg/mL. **(H)** non-infected and treated with **GPs** (1 mg/mL), **(I)** infected and treated with **GPs** (1 mg/mL). **(J-N)** infected and treated with **GPs**+**T6**: **(J)** 0.36 µg/mL, **(K)** 1.63 µg/mL **(L)** 2.95 µg/mL, **(M)** 8.57 µg/mL and **(N)** 15.23 µg/mL.
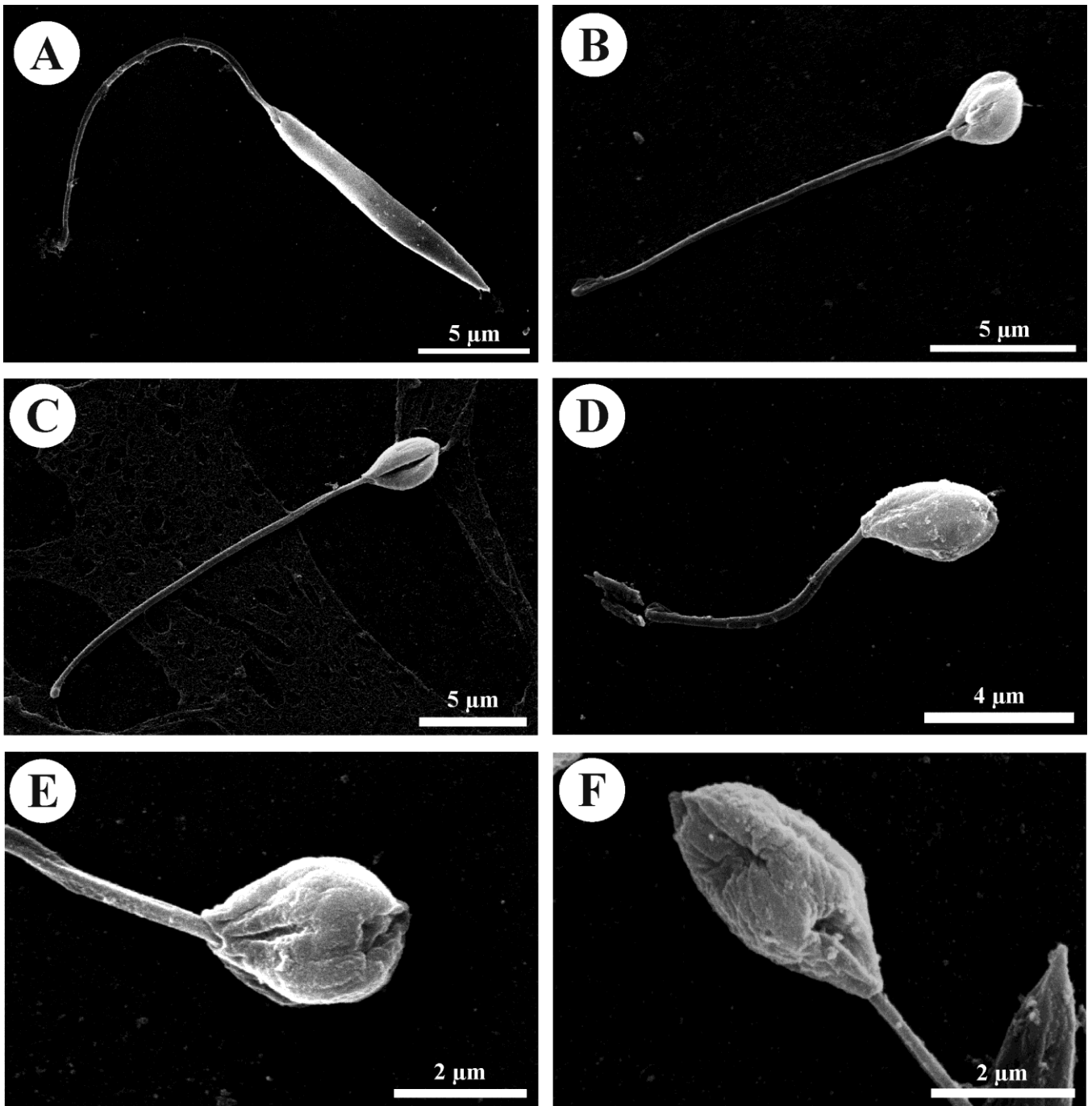
Figure 06. Scanning electronic microscopy of *Leishmania infantum* promastigotes. Cells were treated with **T6** for 72 h. **(A)** untreated, **(B** and **C)** treated with 2.5 µg/mL and **(D-F)** treated with 5.0 µg/mL.
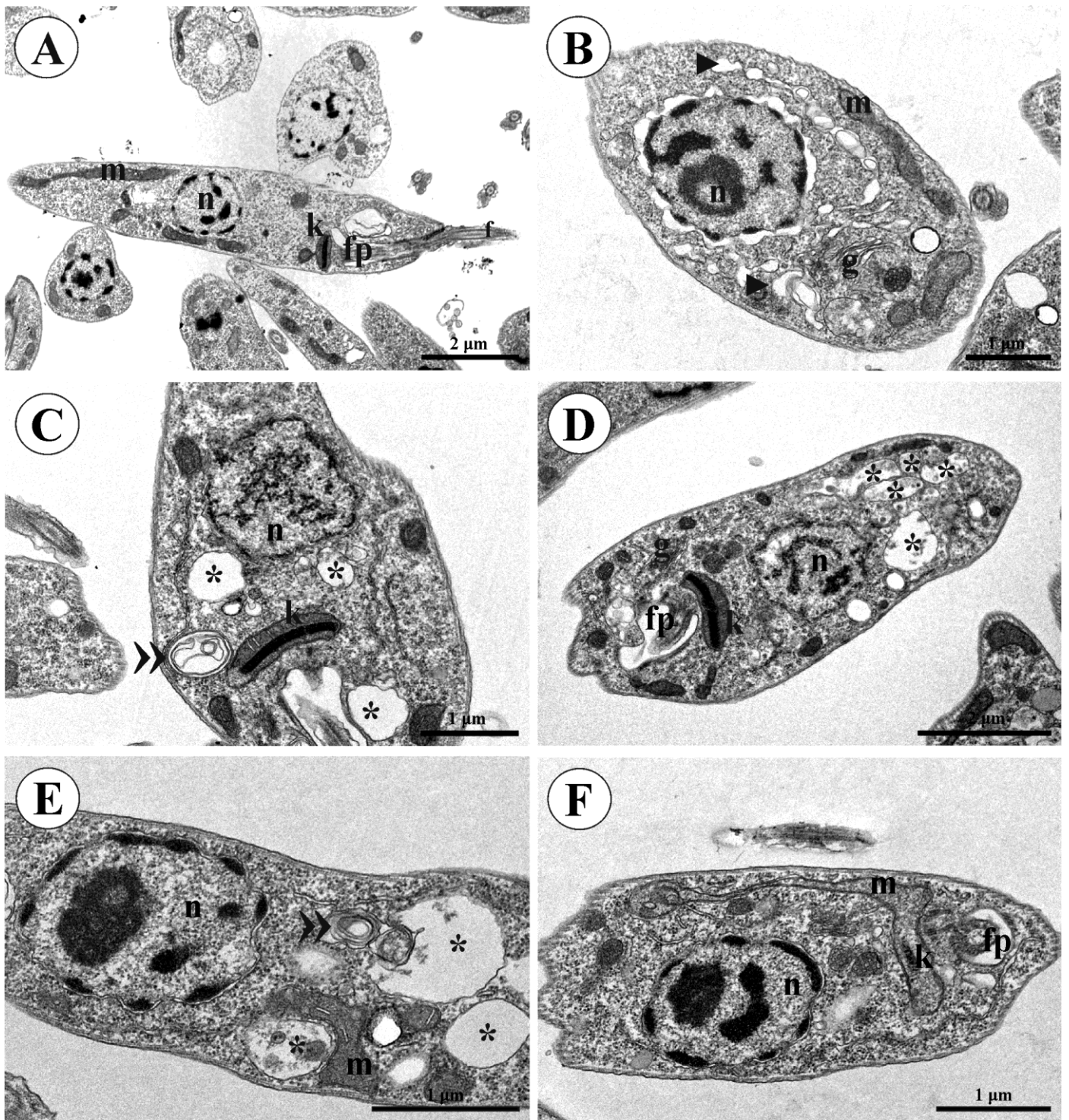
Figure 07. Transmission electronic microscopy of *Leishmania infantum* promastigotes. Cells were treated with **T6** for 72 h. **(A)** untreated, **(B-D)** treated with 2.5 μg/mL and **(E and F)** treated with 5.0 μg/mL. **(n)**: nucleus, **(m)**: mitochondria, **(k)**: kinetoplast, **(fp)**: flagellar pocket, **(g)**: Golgi complex, **(»)** concentric membrane structures, **(*)** autophagic vacuoles and **(▶)** endoplasmic reticulum.
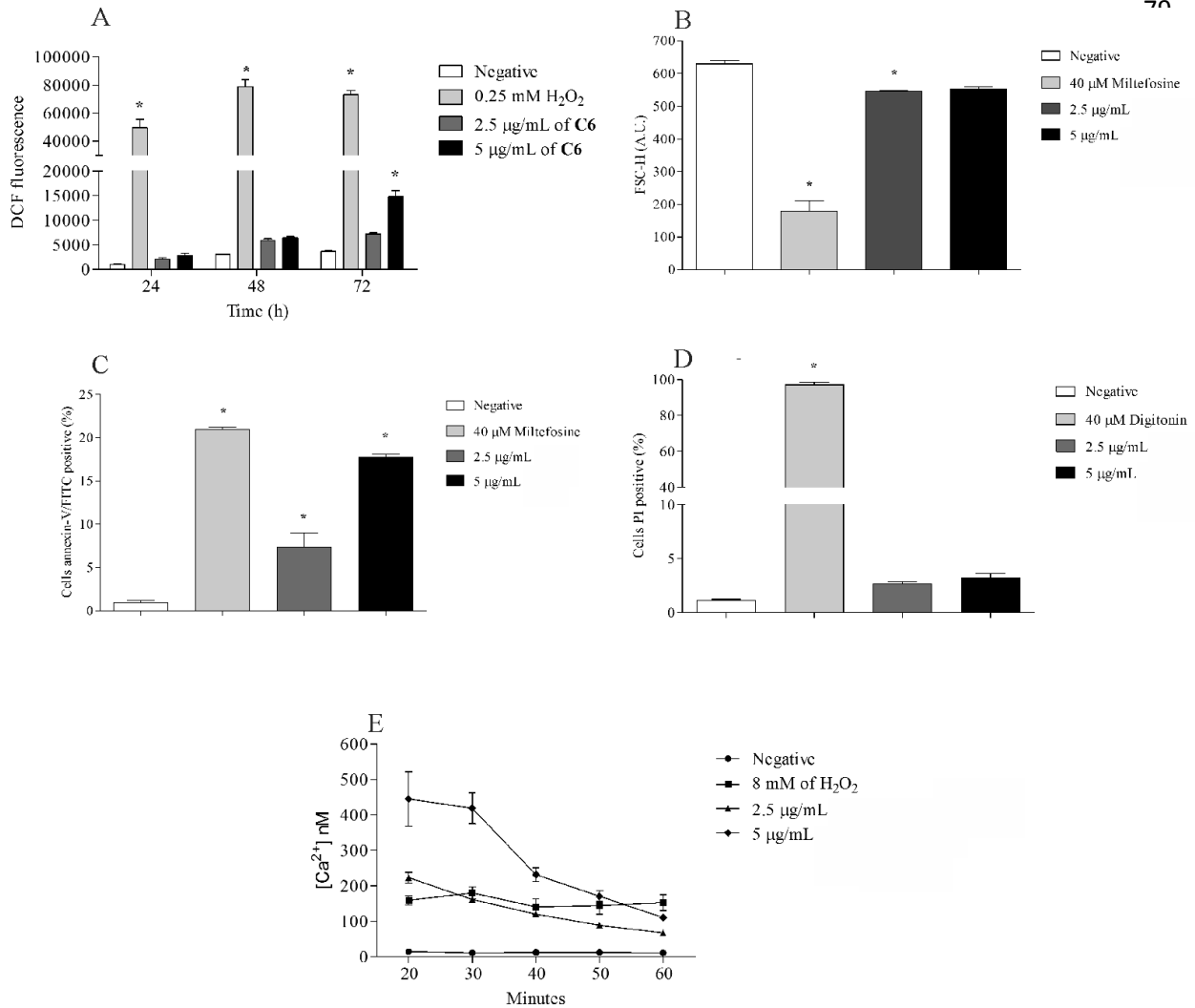
Figure 08. Effects of **T6** in *Leishmania infantum* promastigotes. **(A)** Levels of H_2O_2 in promastigote treated for 24, 48 and 72 h and incubated with H_2DCFDA (10 μM). **(B)** Cell volume in promastigote treated for 24 h **(C)** Exposure of phosphatidylserine in promastigote treated for 24 h and incubated with annexin-V/FITC. **(D)** Plasma membrane integrity in promastigote treated for 24 h and incubated with PI (0.2 μg/mL). **(E)** Intracellular Ca^{2+} levels in promastigotes incubated with Fluo 4-AM (5 μM) and treated for 1 h. (*) Statistically different compared to the untreated control (P<0.05 and n=3).
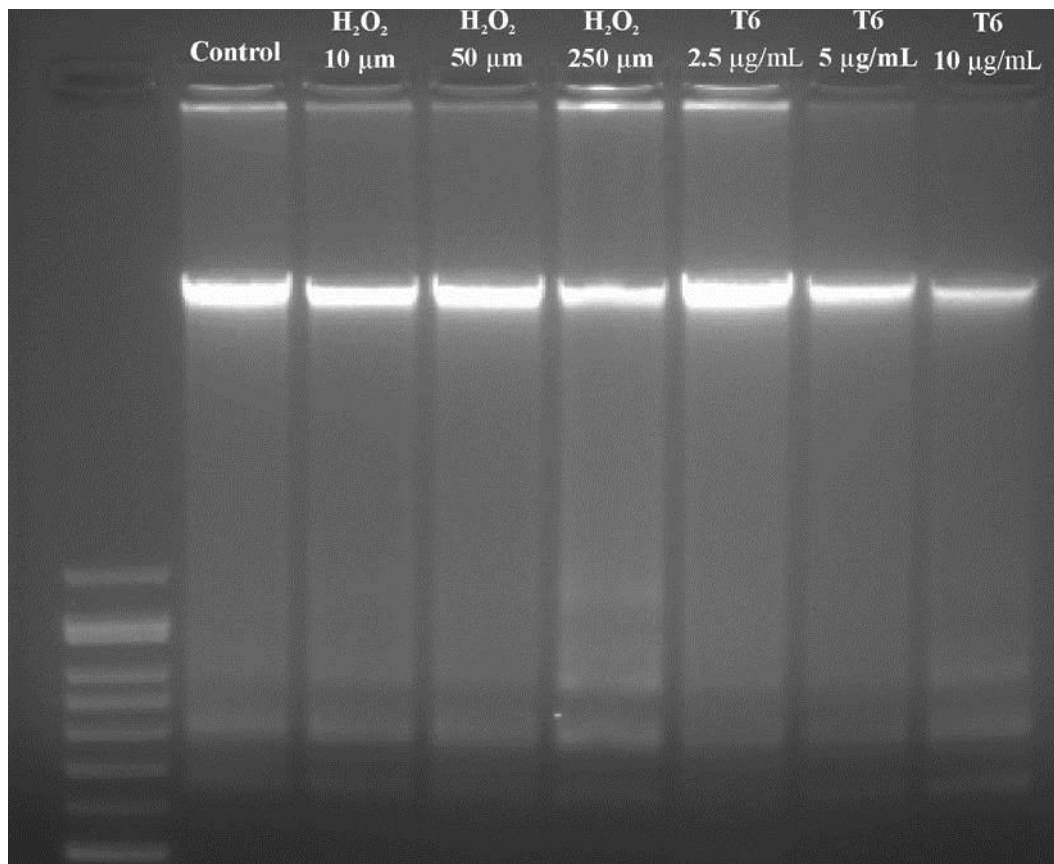
Figure 9. DNA fragmentation in *Leishmania infantum* promastigotes treated with **T6** for 72 h and analyzed by agarose gel electrophoresis. H_2O_2 was used as positive control.